

# ENERGY SHAVER

## A Thermal Energy Storage Device For Air Conditioners

Awardee: James Lester,  
Redstone Engineering Consulting, Inc.  
P.O. Box 340  
Carbondale, CO 81623

Authors: James Lester  
Robert Levenduski  
Rodrigo Fernandez

Grant #: 51332A / 99-16

Grant Amount: \$74,695

Period of Performance: Jan 1, 2000 – Sept 1, 2000

## TABLE OF CONTENTS

<b>1</b>	<b>INTRODUCTION</b>	<b>6</b>
	Statement of Need	6
	Technology Description	7
<b>2</b>	<b>PROJECT ANALYSES</b>	<b>9</b>
<b>2.1</b>	<b>System Modeling</b>	<b>9</b>
2.1.1	Modeling Objective	9
2.1.2	Model Description	9
2.1.3	Modeling Results	11
<b>2.2</b>	<b>Heat Exchanger Modeling</b>	<b>33</b>
2.2.1	Modeling Objective	33
2.2.2	Model Description	33
2.2.3	Modeling Results	36
<b>2.3</b>	<b>Thermal Storage Material Evaluation</b>	<b>37</b>
2.3.1	Evaluation Objectives	37
2.3.2	Evaluation Description	37
<b>3</b>	<b>PROJECT TESTING</b>	<b>41</b>
<b>3.1</b>	<b>Heat Exchanger Testing</b>	<b>41</b>
3.1.1	Heat Exchanger Test Objectives	41
3.1.2	Bench Test Description	41
3.1.3	Heat Exchanger Test Results	41
<b>3.2</b>	<b>PCM Testing</b>	<b>44</b>
3.2.1	PCM Test Objectives	44
3.2.2	PCM Test Description	45
3.2.3	PCM Test Results	46
<b>4</b>	<b>FEASIBILITY ANALYSIS</b>	<b>50</b>
<b>4.1</b>	<b>Technical/Commercial Feasibility</b>	<b>50</b>
<b>4.2</b>	<b>Follow-on Development</b>	<b>51</b>

## ABSTRACT

The Energy Shaver, illustrated below, is a thermal energy storage device for small air conditioners. It uses a salt hydrate to cool the liquid Freon before it reaches the evaporator. This increases cooling capacity and improves efficiency. This simple, low-cost technology could significantly reduce the demand and energy consumption of small commercial and residential air conditioners.

This project supports the development of the technology by conducting system-level and component analyses, and by conducting bench tests of critical components to verify the predicted performance.

The system-level model, which includes environmental conditions, building characteristics, and air conditioner components, was used to investigate the Energy Shaver in a simple retrofit scenario and a replacement scenario. The results are:

- In a replacement scenario, the Energy Shaver reduces peak demand by 25% and energy consumption by 23% by enabling a 4-ton air conditioner to be replaced with a 3-ton air conditioner augmented with the Energy Shaver,
- Only marginal improvement is seen in a simple plug-in retrofit application unless there are significant performance deficiencies in the existing equipment or modifications are made to the evaporator.

Component testing showed the initial, low-cost freon heat exchanger design should be enhanced to provide more area for heat exchange to maximize performance. However, the system-level model included the performance of the original freon heat exchanger design in its predictions, and overall performance was still good.

Follow-on work is required to incorporate a mixing scheme for the salt hydrate to ensure repeatable, long-term performance. Additional follow-on work is required to complete the final packaging with a pricing goal of achieving an immediate payback period in a replacement application.

Keywords: thermal energy storage, energy efficiency, air conditioner

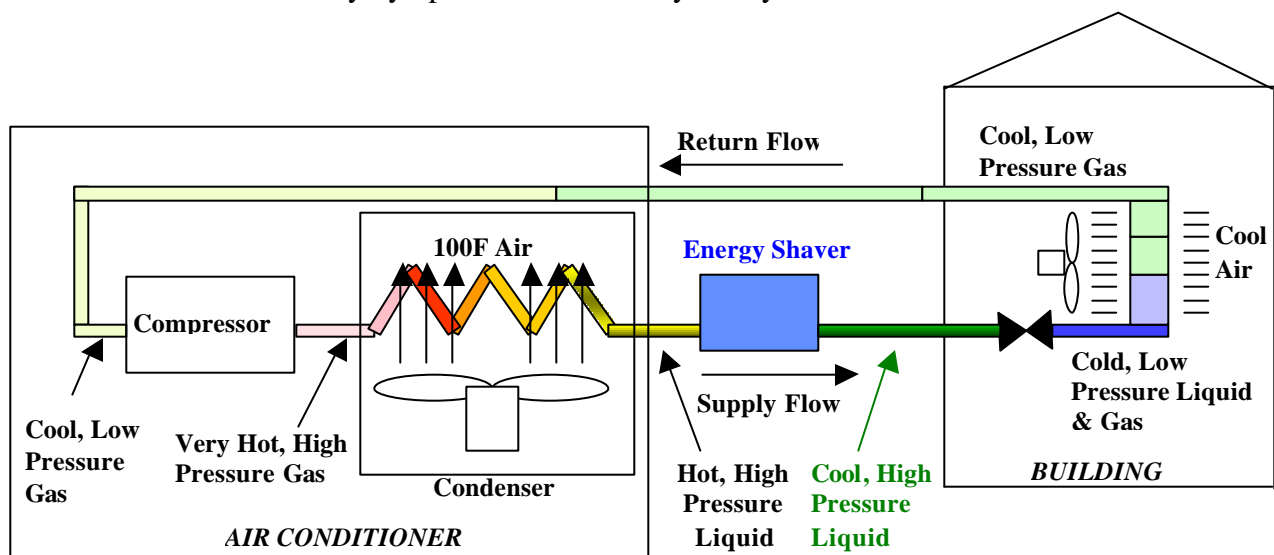


## EXECUTIVE SUMMARY

### Introduction

Electric power demand exceeds supply in many areas of the country during hot summer days. This is a critical problem in California. A large percentage of the peak power demand is driven by air conditioning. The problem is worsening because of growth in the housing market and an increasing percentage of homes with air conditioning.

The Energy Shaver is a thermal energy storage device for use with air conditioners. It is a simple, low cost device that can be used with existing commercial building or residential air conditioners. The Energy Shaver uses a salt hydrate to provide a relatively cool heat sink for the Freon during the hot part of the day. The stored heat is rejected from the salt hydrate to the cool night air to complete the cycle. The Energy Shaver improves the air conditioner's efficiency by up to 30% on hot days. A system schematic is shown below.



### Project Results

#### Analysis

Three analytical models were created to analyze the Energy Shaver: the system model, the Freon-to-hydrate heat exchanger and the hydrate-to-air heat exchanger. The heat exchangers are the most critical components.

The system analytical model was used to consider all important aspects of the system so that the interaction between environmental conditions and various air conditioner components, including the Energy Shaver, could be investigated.

The Freon-to-hydrate model was used to determine the performance of the Freon heat exchanger for the melting process. The hydrate-to-air model was used to determine the performance of the air-side heat exchanger for the freezing process.

#### Modeling Results and Test Results

The following conclusions were drawn from the system modeling results:

- The Energy Shaver offers substantial benefits to small air conditioning systems in a replacement scenario
  - the results show a demand reduction of 25% and an energy savings of 23% when a 4-ton air conditioner is replaced by a 3-ton air conditioner augmented with the Energy Shaver for the test case analyzed
- Modifications to the evaporator is necessary in a simple retrofit application to realize the maximum benefits of the Energy Shaver
- The Energy Shaver is best suited to applications where dehumidification is usually required
  - dehumidification is almost always required because of moisture given off by building occupants
- The melt/freeze cycle can be accomplished with normal ambient conditions

The following conclusions were drawn from heat exchanger component testing:

- The scaled version of the freon-to-salt heat exchanger design did not perform as well as expected. The outlet temperature rose 22°F by the end of the test when the model predicted a rise of 18°F.
- Although the performance is still adequate, additional heat transfer area (longer tubes or extended surfaces) is necessary to meet the stated heat transfer requirements.

The following conclusions were drawn from the salt hydrate tests:

- A nucleating agent must be added to stabilize the refreeze temperature
- Some salt settling occurs with the selected mixture. A loss of thermal capacity of about 5% must be tolerated in the design of the Energy Shaver due to this settling
- Mixing or other measures are needed to maintain long-term thermal performance.

### **Feasibility Analysis**

The modeling and test results indicate the technology is feasible and that the Energy Shaver could provide substantial benefit in a replacement scenario. The user would see immediate cost savings from reduced demand charges and energy consumption in a replacement scenario. It is possible that the smaller air conditioners equipped with the Energy Shaver could cost the same or less than the larger units they replace, thereby offering an immediate payback.

The Energy Shaver would have an enormous impact on the California's energy consumption if it were widely implemented. Most of California has weather that is suitable for using the Energy Shaver and the largest growth areas, which are warmer inland areas, are particularly well suited for it.

### **Follow On Development**

The findings of this effort definitely support follow-on development. Two major areas requiring further development are mixing of the salt hydrate to ensure repeatable, long-term performance and final packaging that enables the Energy Shaver to be integrated with new or existing air conditioning equipment. Top priority should be given to developing the mixing approach as soon as possible.

# 1 Introduction

This report documents the development of the Energy Shaver technology in two key areas: modeling and component testing.

## Statement of Need

Electric power demand exceeds supply in many areas of the country during hot summer days. A large percentage of the peak power demand is driven by air conditioning. The problem is worsening because of growth in the housing market and an increasing percentage of homes with air conditioning.

It is less costly to reduce the peak demand than to build new power plants to meet higher peaks. The Energy Shaver significantly reduces the peak power draw from air conditioners. Utilities across the country can gain additional margin against blackouts and rolling brownouts by installing the Energy Shaver into commercial and residential air conditioners.

California is particularly susceptible to problems associated with peak demand because it has proceeded a long way towards deregulation of the electric industry. The deregulation process has effectively halted construction of new plants because the industry is unsure how deregulation will impact the economics of producing and selling electricity. This has left California with a critical shortage of capacity.

Consequently, the potential benefits of this technology to California electricity ratepayers are significant. Residential users of the Energy Shaver would see reduced energy costs from increased air conditioner efficiency and lower maintenance and repair costs due to reduced operating loads. Small commercial and industrial users would see the same cost reductions plus additional savings from lower demand charges.

Also, because air conditioning loads drive peak demand, widespread use of the Energy Shaver may eliminate the blackout threats and the associated non-productive periods. Widespread use of the Energy Shaver will ease the power crunch until new power plants come on-line. Peak demand is projected to continue growing because of population growth in the warmer areas of California. Compounding the problem is the fact that the percentage of new homes with central a/c is increasing, which will also increase summer time energy demands.

There are two markets for the Energy Shaver. One is the energy services market that provides low cost, highly reliable, increased efficiency cooling solutions that provide savings on utility bills to business and residential customers. The other is Demand Side Management (DSM) programs operated by utilities that have pressing peak demand problems that must be resolved.

## Technology Description

The Energy Shaver is a thermal energy storage device for use with air conditioning systems. It is a simple, low cost device that can be used with existing commercial building or residential air conditioners. The Energy Shaver improves the air conditioner's efficiency on hot days. Efficiency improvement can approach 30% for rooftop units that get significantly hotter than the ambient air temperature because of their rooftop location. The hotter the day, the greater the energy savings.

In a replacement scenario, the additional cooling capacity provided by the Energy Shaver enables a smaller unit to be installed. This allows the smaller air conditioner to run more efficiently near its design point while the Energy Shaver provides the extra capacity when needed to meet the peak cooling demand.

The Energy Shaver uses a salt hydrate to provide a relatively cool heat sink for the Freon during the hot part of the day. Late in the day, or at night, when the ambient air temperature has decreased sufficiently, the stored heat is rejected from the salt hydrate to the ambient air. Other systems that cool the condensed Freon, such as a mini-cooling tower (water evaporation tower), are complex, have high first costs and high maintenance costs. The same is true of ice storage systems that make ice at night and use it during the day to provide cooling. The Energy Shaver is based on inexpensive materials and fabrication methods that make it economically feasible. The high thermal storage capacity of the salt hydrate permits a highly reliable, low maintenance, compact system that can be easily incorporated into existing HVAC systems or integrated into original equipment by the manufacturers. These factors make the Energy Shaver an innovative and practical device.

A system schematic is shown in Figure 1-1. Fundamentally, the Energy Shaver lowers the heat rejection temperature of the refrigeration cycle. Heat is rejected to the salt hydrate when the ambient temperature is higher than the salt hydrate temperature. The stored heat is rejected when the ambient temperature is less than the salt temperature. Efficient heat storage is accomplished through a phase change (melting). Based on first principles of thermodynamics and the thermodynamic properties of R-22 refrigerant, a 1% increase in efficiency will result from every 2°F of condensate cooling. The improved heat transfer of the Energy Shaver compared to standard condensers will achieve an additional efficiency improvement of 10% at 80°F. Figure 1-2 shows the efficiency improvement versus ambient air temperature. Studies have shown that the effective air temperature for rooftop air conditioners routinely approaches 130°F. It is noted that the overall efficiency improvement is slightly less than indicated when the fan power necessary to reject the heat at night is considered. The fan power is a small percent of the savings.

Thermal energy storage systems that use salt hydrates are not new. They have been used for many years in solar heating systems. However, our method of implementing energy storage on the hot (condenser) side of an air conditioner is new. We have filed a patent application because a thorough patent search confirmed no similar approach was patented.

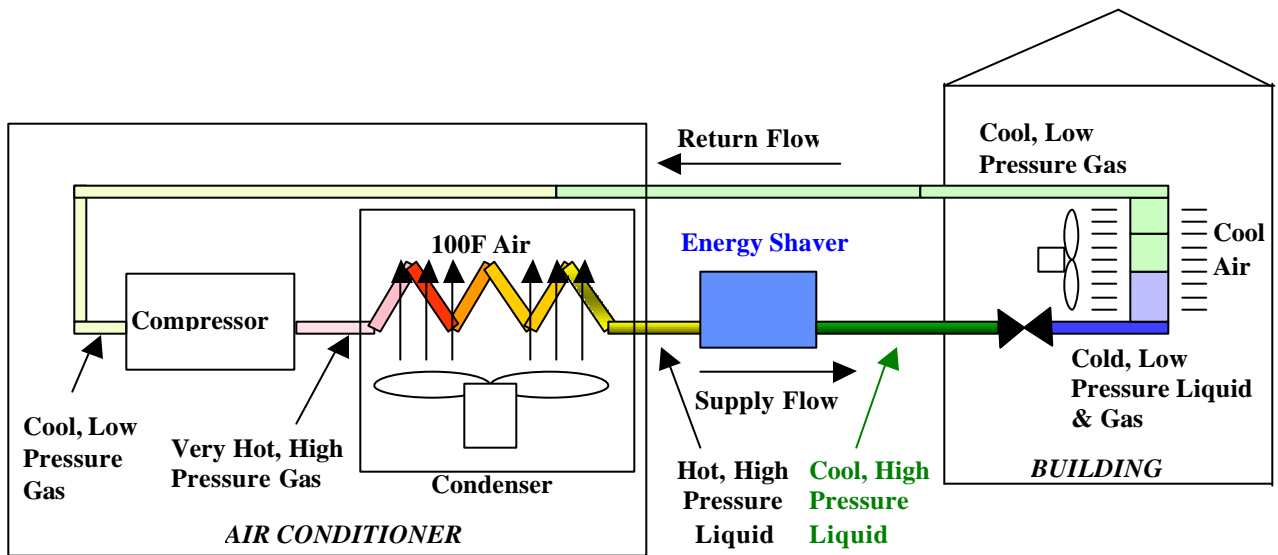


Figure 1-1. System Schematic Showing Operation of the Energy Shaver

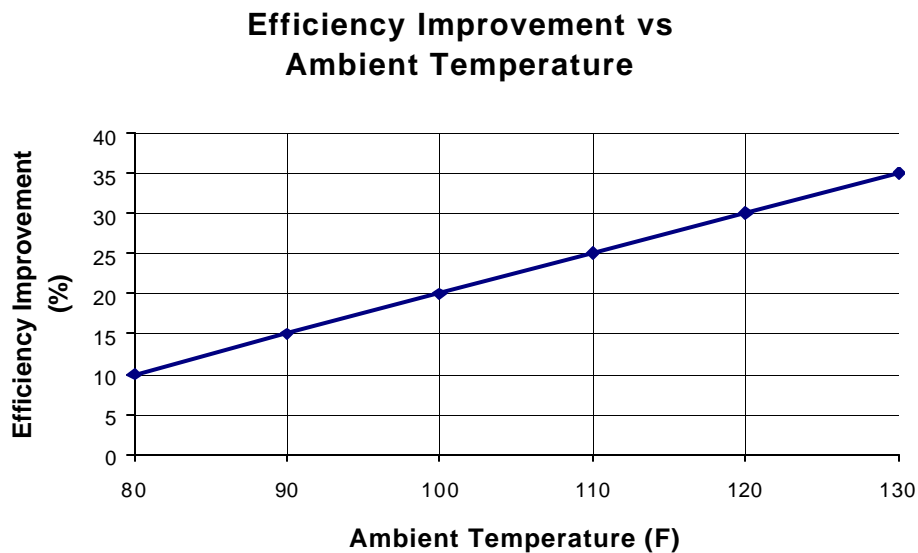


Figure 1-2. Efficiency Improvement versus Ambient Temperature

The project goals are to advance the development of this technology to the point where it's feasibility can be determined, and potentially beyond. The specific project tasks are:

- Develop an analytical system model to investigate the Energy Shaver device
- Develop an analytical model of the salt hydrate container and heat exchangers
- Investigate materials choices for the container and salt hydrate
- Conduct component testing to validate assumptions of the models, specifically,
  - bench testing of the Freon-to-hydrate heat exchanger
  - cycle testing and investigation of salt hydrates.

## 2 Project Analyses

### 2.1 System Modeling

#### 2.1.1 Modeling Objective

The objective of creating the system analytical model was to create an analysis tool that considered all important aspects of the system so that the interaction between environmental conditions and various air conditioner components, including the Energy Shaver, could be investigated. This would allow the impact of the Energy Shaver on the overall system-level performance to be predicted. The model could also be used to conduct parametric analyses necessary for system optimization.

#### 2.1.2 Model Description

##### 2.1.2.1 Modeling Approach

An earlier study concluded the Energy Shaver was best suited for packaged or split air conditioning systems of five tons or less. Consequently, the system model was created specifically for systems of this size that use capillary tubes as the expansion device. However, the model could easily be modified to accommodate larger systems with a thermostatic expansion valve.

The system model is a dynamic simulation of the complete system. It was written in the rather archaic Fortran language to be compatible with a linkable fluid properties program called Gaspak. The model makes several calls to the Gaspak program to calculate refrigerant (R-22) properties for each iteration of the model.

The model was kept fairly simple because the emphasis was on the comparison of performance with and without the Energy Shaver, and not its absolute accuracy in predicting the system's performance. As an example, an algorithm derived from weather data was used to determine the outdoor temperature as a function of time instead of actual data from various weather stations. This approach was adequate for the performance comparison with and without the Energy Shaver.

As mentioned previously, the model is a dynamic simulation of the complete system. This means that each component in the system is given inputs, calculates a response to those inputs based on its transfer function, and creates an output. The inputs and outputs of each component are appropriately linked to other components to achieve a closed loop response. The model is iterated in small time increments with initial conditions and proceeds through a 24 hour cycle to analyze a complete day. For example, initial conditions at midnight might be outdoor temperature at 70°F, building at 70°F, thermostat setting at 80°F and air conditioner off. As the model runs, the outdoor temperature would first cool until early morning and then rise. The building temperature would rise with the outdoor temperature and internal heat load. It would eventually exceed the thermostat setting at which point the air conditioner would turn on. The circulating air blower would then circulate the cool air through the building, eventually cooling it to below the thermostat setting and turning off the air conditioner. With the air

conditioner off, the building would warm again and the air conditioner would eventually turn back on. This is repeated for a 48-hour cycle to establish equilibrium operation and to eliminate errors that may be introduced by the initial conditions. Figure 2-1 shows the system schematic and model's nodes of interest.

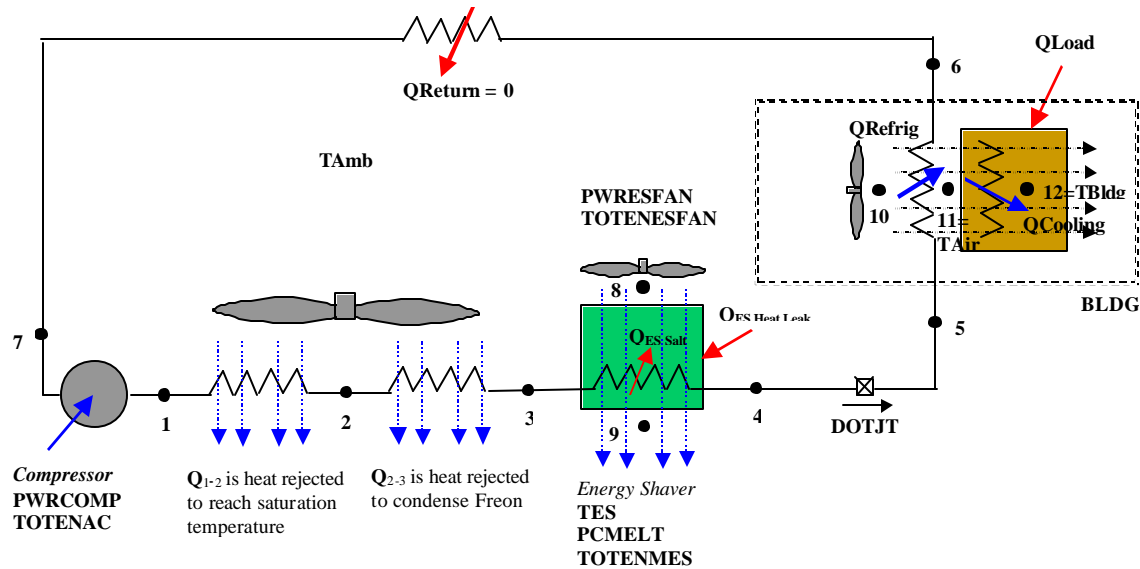


Figure 2-1. System Model Schematic with Key Program Variables Identified

#### 2.1.2.2 Component Descriptions

A reciprocating compressor was chosen for the model. It is straightforward to model and the predicted performance can be compared to readily available performance curves. Most small packaged and split air conditioners now use scroll compressors, so the model has been constructed to be easily modified in the future to incorporate the scroll compressor performance characteristics.

The condenser was modeled as a heat exchanger with a fixed temperature difference between the ambient air and exiting condensate. This is a simplified approach, so the temperature difference was made an input variable so that parametric modeling could be done for the condenser.

The Energy Shaver model contains a fan, a Freon-to-hydrate heat exchanger, a hydrate-to-air heat exchanger and a mass of salt with the appropriate thermodynamic properties. The Energy Shaver's design airflow was calculated based on heat rejection temperature and time requirements. A matching fan and associated power was determined from a standard product sheet. The hydrate-to-air heat exchanger was modeled using the Effectiveness-NTU method. The effectiveness value was made an input variable for parametric analysis purposes. The baseline value was derived from detailed heat exchanger calculations for the baseline configuration. The Freon-to-hydrate heat

exchanger was initially modeled using the Effectiveness–NTU method, but was later changed to an algorithm that replicated the component test results. This algorithm replicated the effect of the increasing liquid thickness around the freon heat exchanger as the salt melted, which resulted in an increasing freon exit temperature versus time.

The expansion device was modeled as a capillary tube. Most small units use capillary tubes to expand the fluid so this was the most appropriate choice. The flow characteristics (flow rate as a function of inlet pressure and temperature) were taken from flow curves of a 4-ton split system.

The evaporator and blower were also modeled using the Effectiveness–NTU method. The blower was sized according to ARI Standards to match the size of air conditioner modeled. The heat exchanger effectiveness was based upon performance data from a 4-ton split system. The effectiveness was made an input variable for parametric analysis purposes. The return air conditions (dry and wet bulb) were initially set in accordance with ARI standards for rating of air conditioners. The blower power was not included in the analysis.

### **2.1.3 Modeling Results**

#### **2.1.3.1 Model Verification**

The first task was to verify the model produced reasonable results for a standard case. We chose to run a case with a 4-ton air conditioner cooling a building that had a peak load of 4 tons during the day. From this, we could look at the energy balance of the system as a whole as well as review the performance of each component. The graphs that follow are a standard set for all runs. They will each be discussed in detail here to lay a foundation for discussion of all graphs that follow. Additional graphs detailing the performance of the Energy Shaver will be included and described later. The following values for the key variables in the model were used for the verification run:

- QACMAX (a/c max cooling at 95°F DB outdoor air temperature) = 13.33 BTU/s (4 tons)
- QAMBMAX (max heat load at 95°F outdoor temperature) = 13.33 BTU/s
- TMEAN (mean outdoor temperature) = 80°F
- TRANGE (temperature swing from TMEAN) = 15°F (this gives maximum outdoor temperature of 95°F and minimum outdoor temperature of 65°F)
- TSET (building thermostat setting) = 80°F (this is consistent with ARI Standard 210/240 for rating unitary air conditioners). Dry return air was assumed for this case to ensure no condensation occurred.
- BLDGAIR (indoor blower circulating air flow) = 1800 CFM (450 CFM/ton max per ARI Standard 210/240)

Figure 2-2 shows the building data. The output parameters are TAMB (outdoor temperature), TBLDG (indoor temperature at the thermostat), TAIR (supply air temperature), QAMB (conduction heat load), QSOLAR (solar heat load), and QLOAD (total heat load = the sum of QAMB and QSOLAR).

The outdoor ambient temperature (TAMB) is calculated as a sine function. It reaches a maximum value of 95°F at 15:00 hours (3:00 pm) and a minimum value of 65°F at 03:00 hours (3:00 am). This is a simplified approach, but is representative of actual temperatures recorded from weather stations. The building thermostat is set at 80°F and has a  $\pm 1^\circ\text{F}$  deadband. Consequently, the air conditioner turns on when the indoor temperature reaches 81°F and turns off when it reaches 79°F. The deadband is clearly noticeable on the TBLDG data. The supply air (air exiting the evaporator) is shown as TAIR. When the air conditioner is off, the temperature is set to the building temperature. The model calculates the air exit temperature when the air conditioner is on. This data indicates the duty cycle of the air conditioner. Note that during the time of highest heat load (QLOAD) the air conditioner runs constantly yet it barely lowers the building temperature. This indicates a balance has been achieved between the air conditioner's cooling capacity and the peak heat load. Because no condensation is occurring in the supply air, this verifies the model is balanced and is producing reasonable results. The total heat load (QLOAD) has been divided into solar (QSOLAR) and temperature (QAMB) components. This was done so the outdoor temperature could be changed without affecting the solar load.

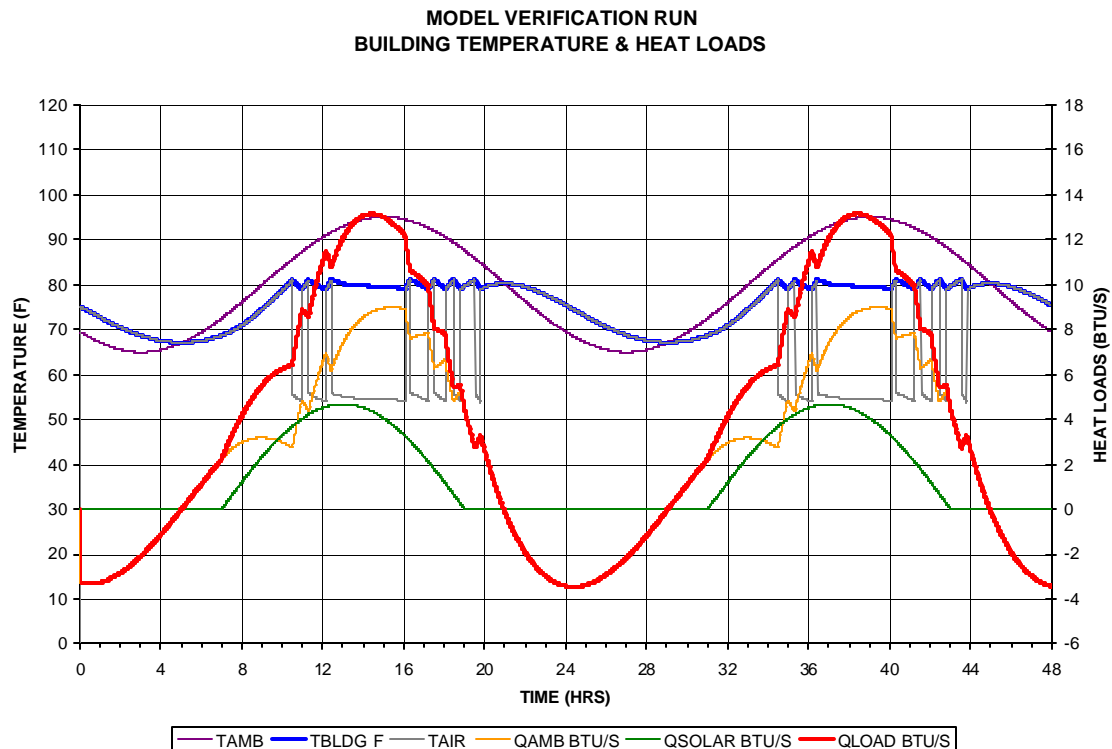


Figure 2-2. Building Temperature and Heat Loads

Figure 2-3 shows that no condensation is occurring. The total cooling produced by the air conditioner (QREFRIG) and the sensible cooling (QCOOLING) are the same. These values will differ if condensation occurs, as will be seen in later graphs.

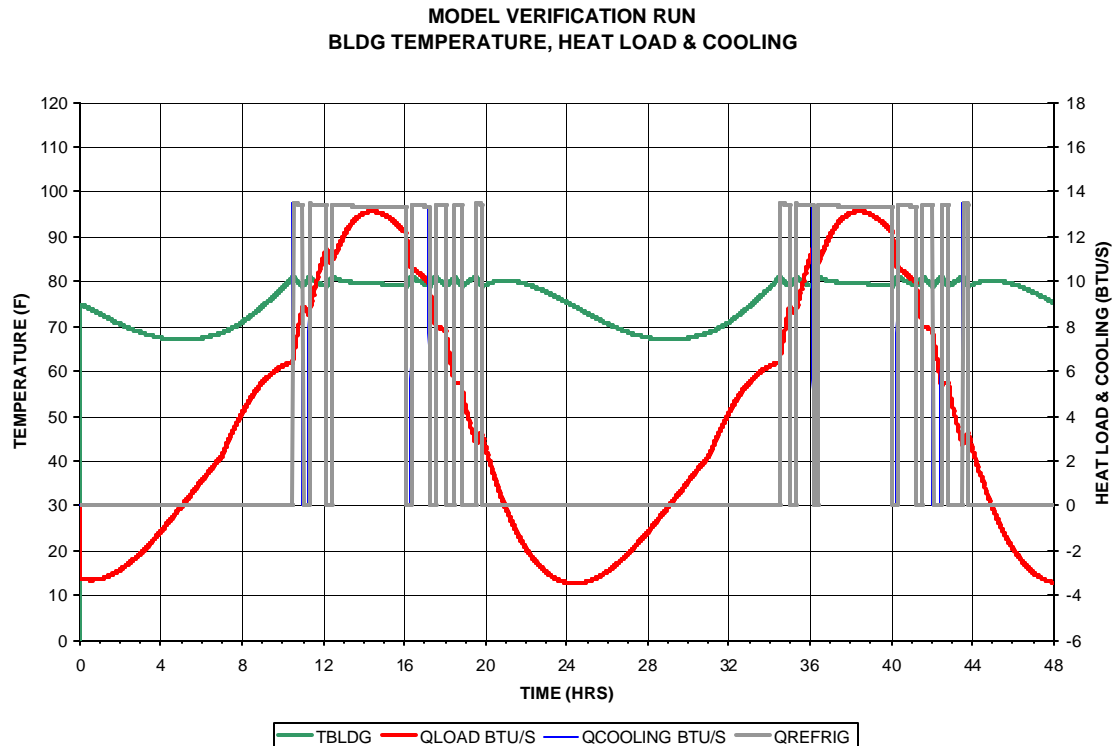


Figure 2-3. Air Conditioner Total and Sensible Cooling

Figure 2-4 shows the node temperatures of the air conditioner. Refer to figure 2-1 for node locations. The temperatures show that the air conditioner model is producing reasonable results. The outlet temperature from the compressor (TEMP1) is well above ambient and the temperature exiting the condenser (TEMP3, which overlays with TEMP4) is 15°F warmer than the ambient air temperature. The evaporator temperature (TEMP5) is approximately 45°F, which is consistent with a properly charged unit.

Figure 2-2 shows the supply air (TAIR) is normal at 55°F. The model does not currently add heat to the return line between the exit of the evaporator and the inlet to the compressor, although it can be easily added in the future. As a reminder, when the air conditioner is not on, the node temperatures are set to the ambient temperature.

The air conditioner's high and low pressures and mass flow rate are also reviewed to ensure the air conditioner model is producing reasonable results. Figure 2-5 shows the high side operating pressure (PRES(1)) varies as expected with ambient temperature. The graph also shows the increase in mass flow (DOTJT) through the capillary resulting from the higher supply pressure. As a result of the higher flow, the low pressure (PRES(7)) also increases to enable the compressor to match the higher flow through the capillary. These results give confidence that the model is producing reasonable results.

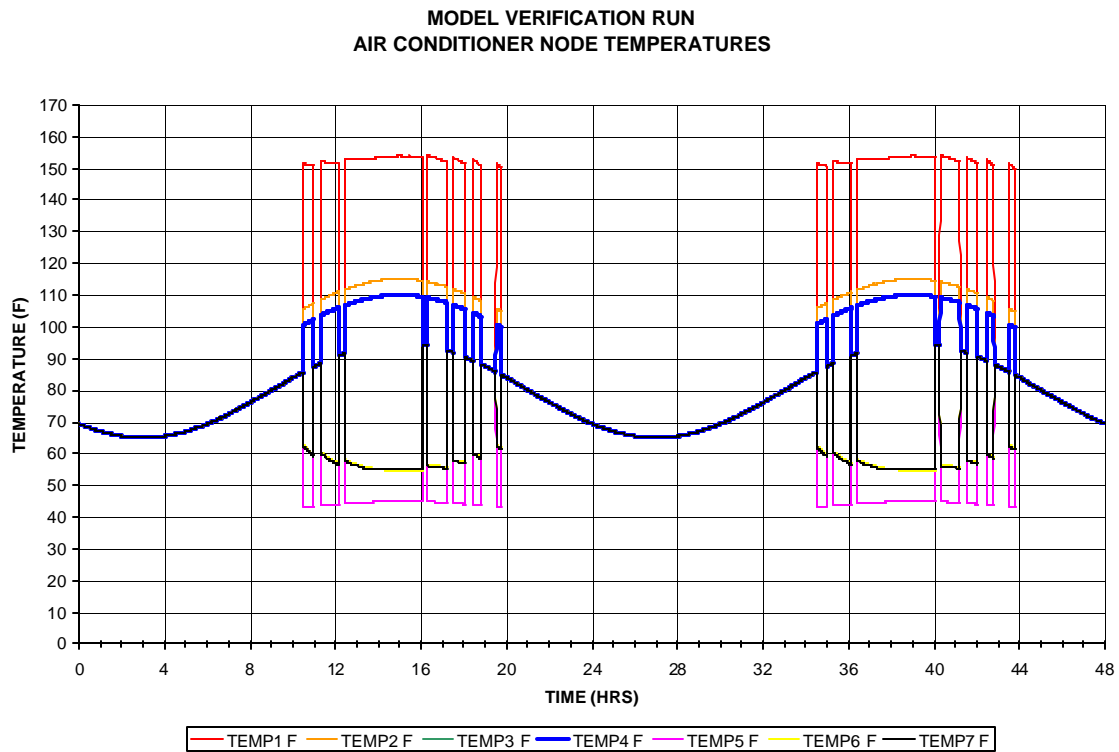


Figure 2-4. Air Conditioner Node Temperatures

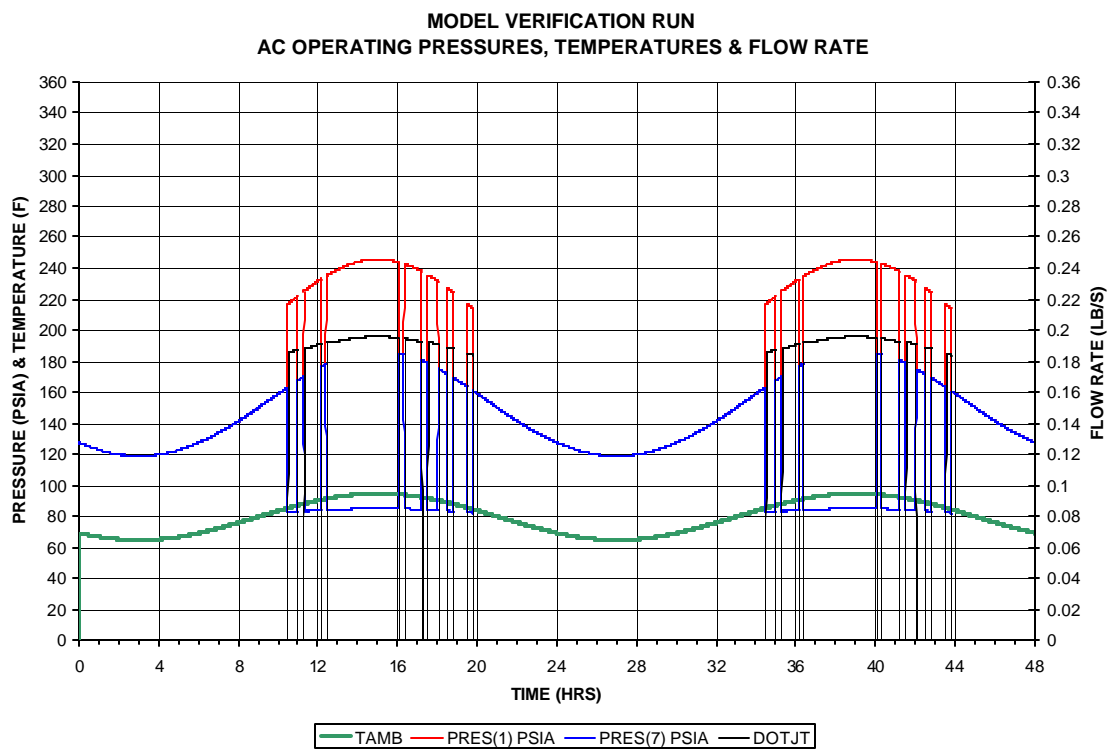


Figure 2-5. Air Conditioner Pressures and Flow Rate

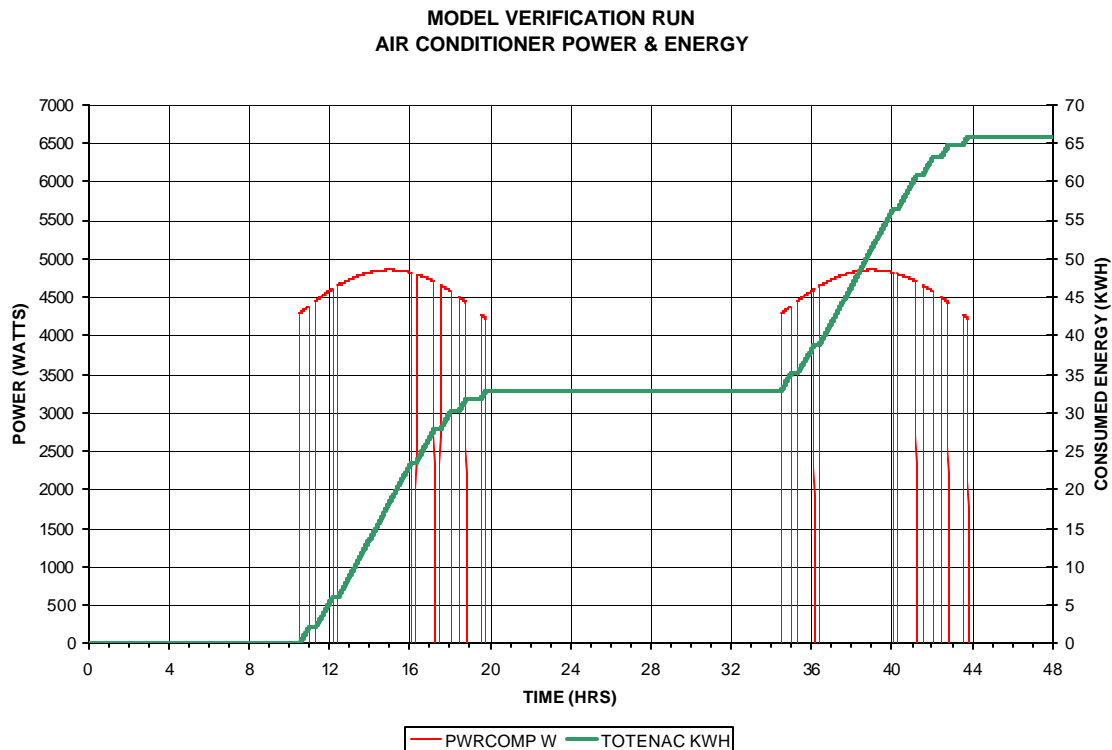


Figure 2-6. Air Conditioner Demand and Energy Consumption

Ultimately, the model must compare the air conditioner's power consumption and demand with and without the Energy Shaver to determine if savings are realized. Figure 2-6 shows the demand (PWRCOMP) and energy consumption (TOTENAC). These numbers are calculated by multiplying the compressor power (calculated in the model based on flow work) by an efficiency factor to account for electrical inefficiencies and the condenser fan. The compressor flow work was multiplied by a factor of 2 to arrive at total system power. This gave an overall efficiency of approximately 1.2 kW/ton, which is within range of standard equipment. This factor remained constant for all runs.

Based on these results, we conclude that the system model is producing reasonable results for the verification case. The model can be used with confidence to compare system performance over a range of environmental conditions, with and without the Energy Shaver.

#### 2.1.3.2 Baseline Case

The baseline case establishes a performance baseline to which the effects of the Energy Shaver can be compared. The baseline case differs from the verification case in that the same 4-ton air conditioner is put into a system more representative of actual use. The three major differences are: 1) the maximum heat load is lowered from 4 tons to 3 tons at 95°F to account for typical oversizing of installed units, 2) the thermostat setting is lowered from 80°F, the ARI rating standard, to 74°F, which is a more typical setting for homes and businesses, and 3) the return air is assumed to have a 64°F wet bulb

temperature instead of the ARI rating standard of 67°F. The modeling results are shown in the following graphs.

Figure 2-7 shows the building temperature and heat loads. The outdoor ambient temperature remains the same from the verification case. Note however, that the building temperature is not maintained at the thermostat setting of 74°F. This is due to two factors. First, the conduction portion of the 3-ton load is achieved at 95°F when the building temperature is at 80°F so having the building thermostat set at 74°F increases that portion of the heat load. Second, condensation occurs during cooling of the return air because the dew point is 58°F. This effect can be seen in Figure 2-8 and will be discussed shortly. Also note the duty cycle. The air conditioner runs constantly from 11:00 to 19:00 hours. This illustrates the fact that lowering the thermostat setting substantially increases energy consumption of air conditioners.

The effect of condensation on cooling capacity is shown in Figure 2-8. The air conditioner's total cooling capacity (QREFIG) remains the same as in the verification case, but the cooling available to cool the building (sensible cooling, QCOOLING) is substantially reduced. Compare this graph to figure 2-3. Also note that the reduced sensible cooling resulted in a slightly warmer supply air temperature, shown in Figure 2-7.

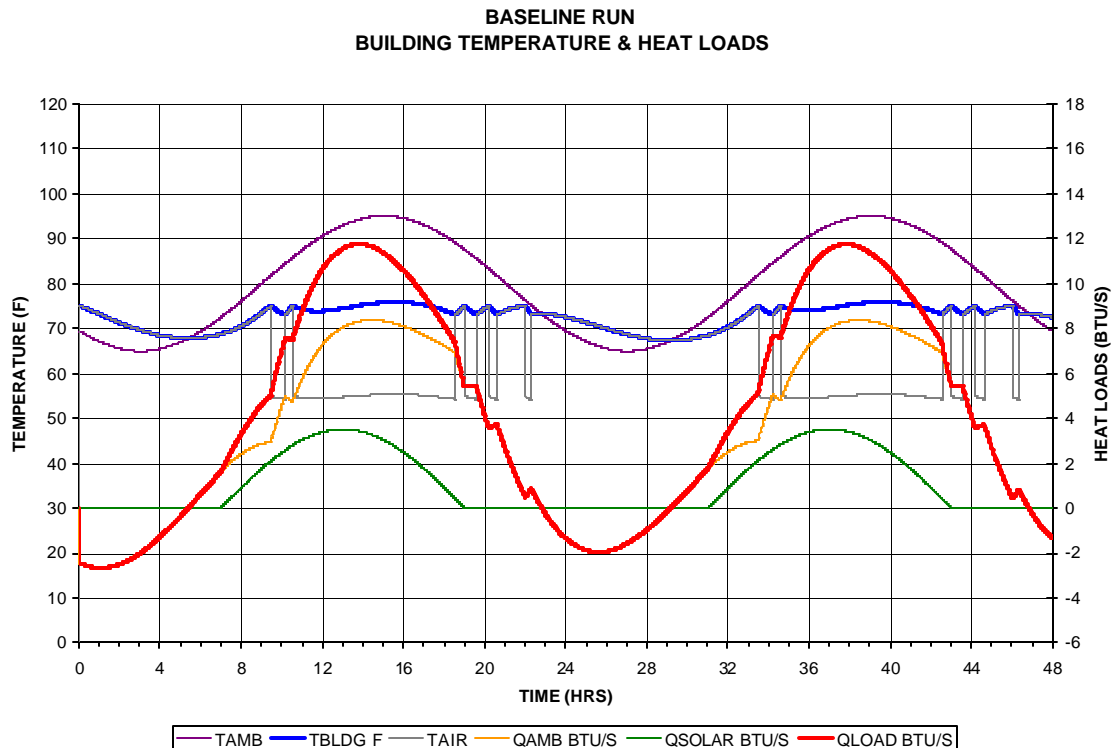


Figure 2-7. Building Temperature and Heat Loads

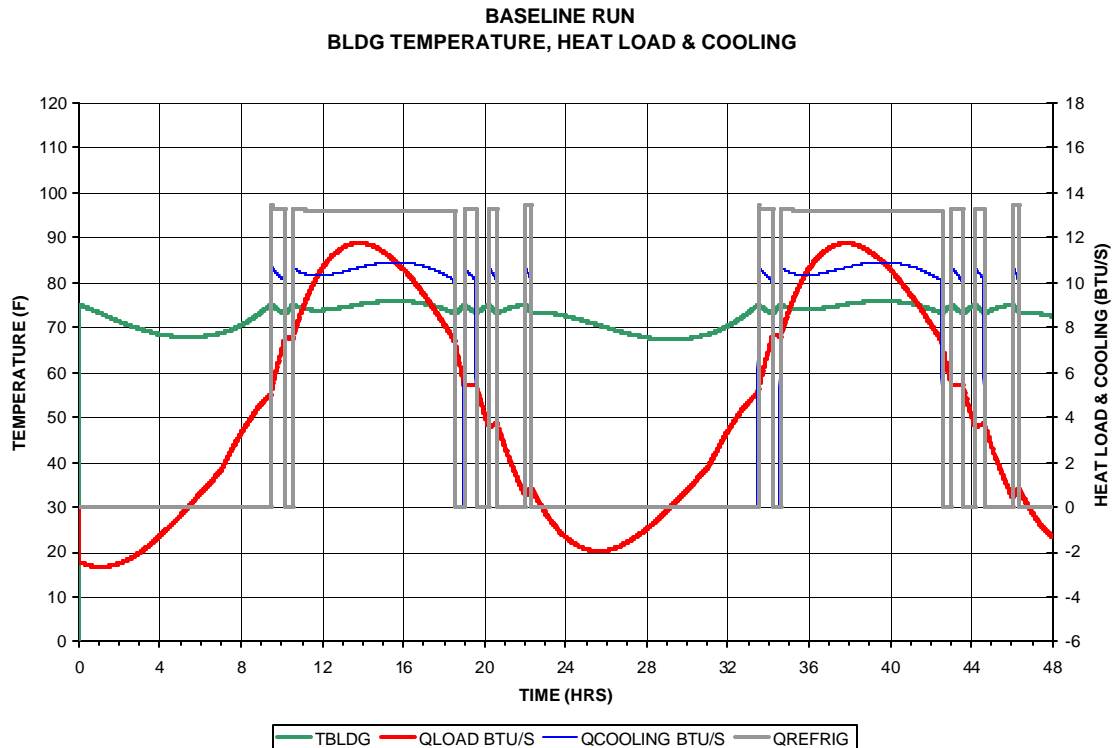


Figure 2-8. Air Conditioner Total and Sensible Cooling

Figure 2-9 shows the air conditioner node temperatures. Since the same air conditioner was used as in the verification case, no differences are seen in TEMP 1 through 5. However, TEMP 6 and TEMP 7 are slightly lower in this case because the building return air is colder and it doesn't superheat the Freon exiting the evaporator as much.

Figure 2-10 shows the air conditioner's pressures and mass flow. The pressures and flow are identical to the verification case because the same air conditioner was used and there were no changes in the temperatures of nodes 1 through 5. Compare this to figure 2-5.

Figure 2-11 shows the air conditioner's energy consumption and demand. The demand remains virtually unchanged, as expected, because there are no changes to the high-pressure side and the slightly lower return temperature has very little effect on overall performance. However, the energy consumption is substantially larger than in the verification case. This is a direct result of the air conditioner running longer. The increased operating time becomes obvious when comparing figures 2-11 and 2-6. This illustrates the energy impact of lowering the thermostat setting and dehumidifying the air.

The results of the verification case and the baseline case are consistent with expectations and thus give confidence that the model can be used to investigate the impact of the Energy Shaver.

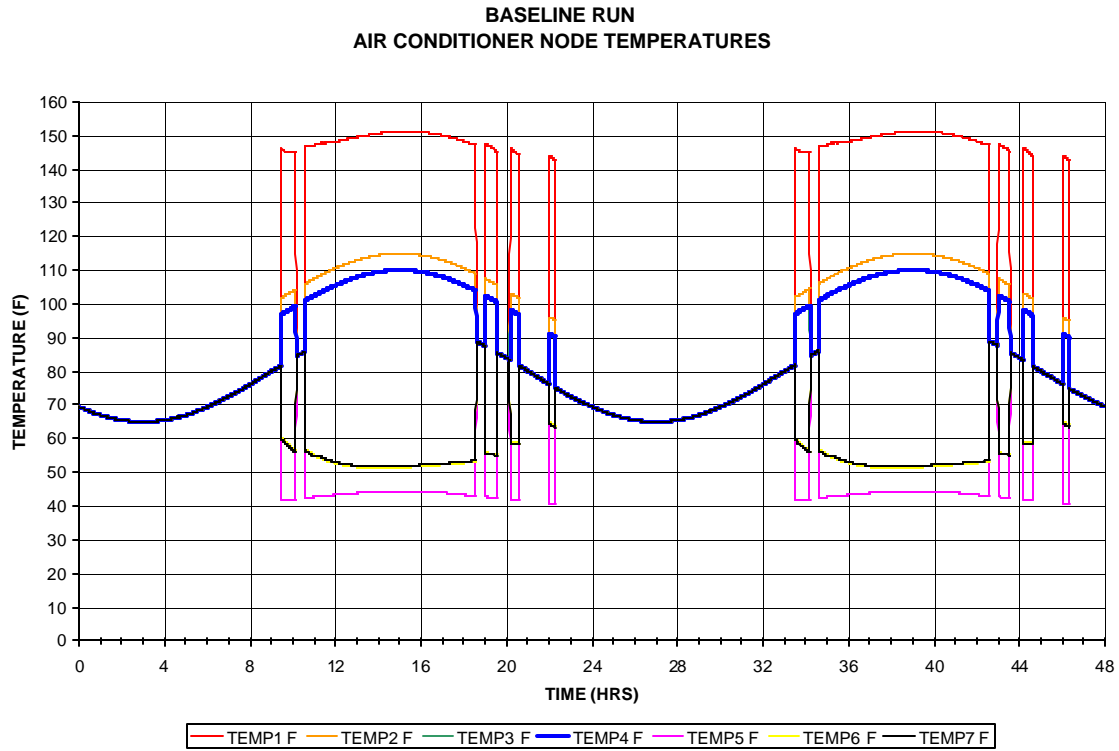


Figure 2-9. Air Conditioner Node Temperatures

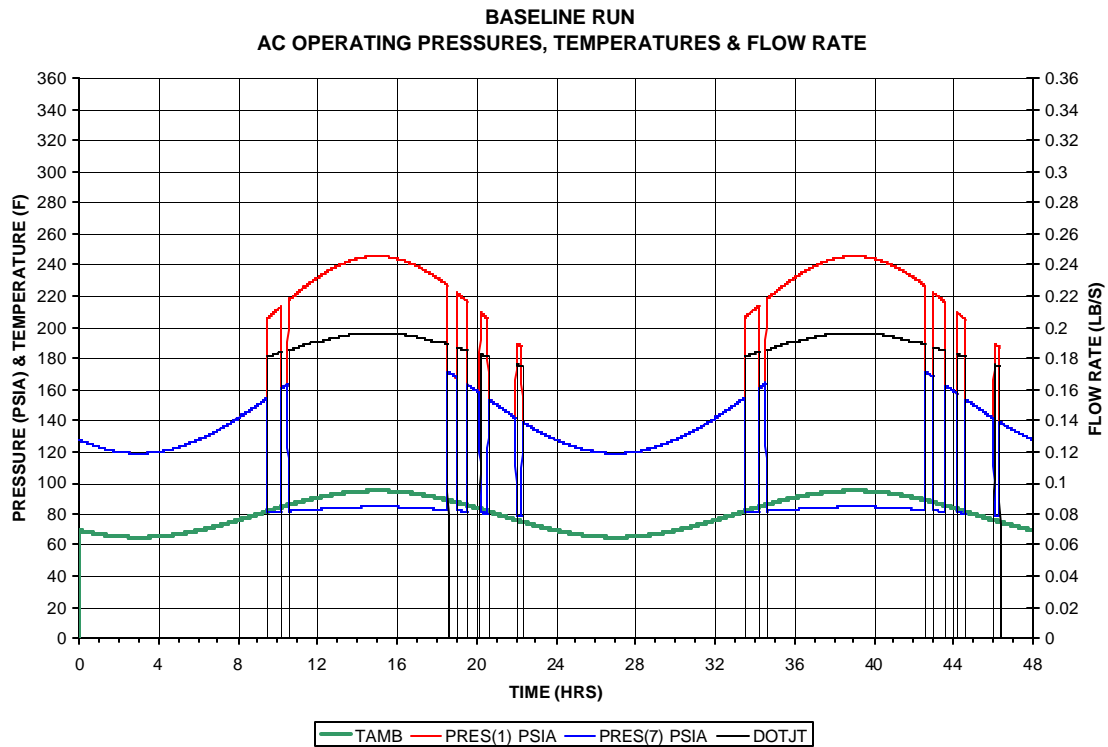


Figure 2-10. Air Conditioner Pressures and Flow Rate

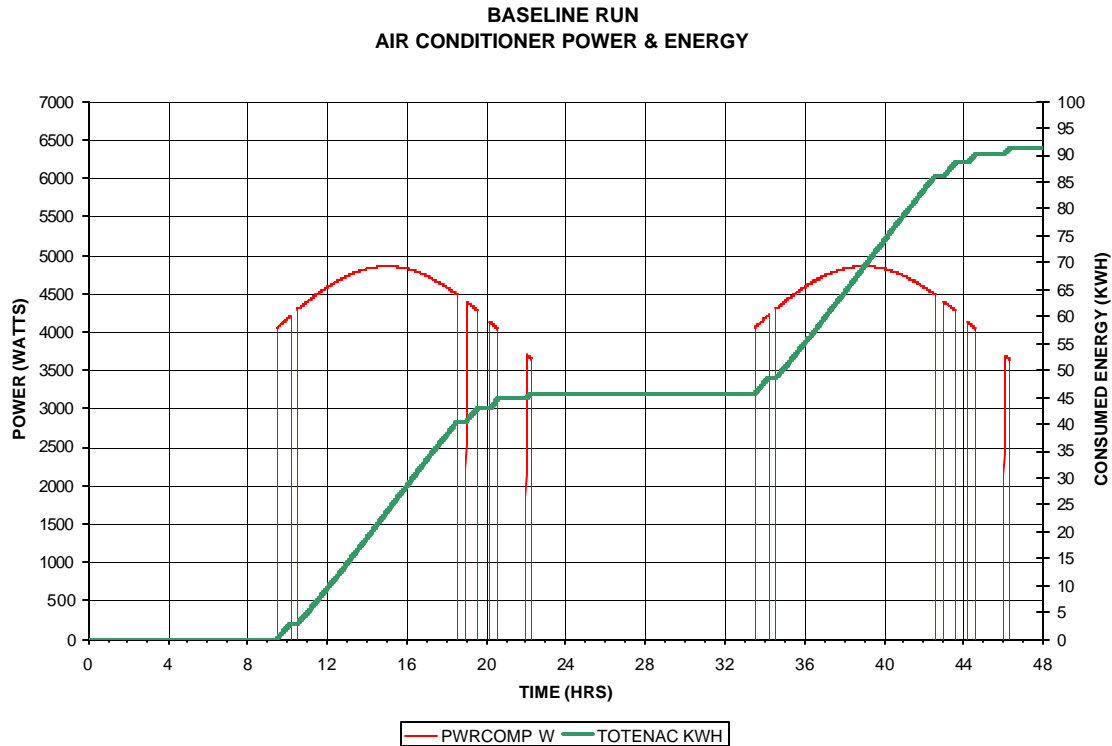


Figure 2-11. Air Conditioner Demand and Energy Consumption

### 2.1.3.3 Simple Retrofit Case

The first case that includes the Energy Shaver is the simple retrofit case. Here, the Energy Shaver is added to a properly functioning air conditioner. The new input parameters for the Energy Shaver are:

- TMELT (salt hydrate melt temperature) = 86°F
- MES (weight of salt in Energy Shaver) = 350 lbs
- CPLIQ (heat capacity of liquid hydrate) = 0.795 BTU/lb-F
- CPSOL (heat capacity of solid hydrate) = 0.401 BTU/lb-F
- CFMESFAN (Energy Shaver fan flow) = 2500 CFM
- CPMELT (effective heat capacity of melting salt) = 4.5 BTU/lb-F

Figure 2-12 shows the building data. The performance is slightly improved compared to the baseline case shown in figure 2-7. With the Energy Shaver, the air conditioner cooled the building nearly one degree cooler during the hottest part of the day. This was a consequence of providing cooler supply air to the building.

Figure 2-13 shows the total and sensible cooling capacity. The Energy Shaver significantly increased the total cooling capacity of the air conditioner compared to the baseline case, figure 2-8. The total cooling capacity increased from 13.2 to 15.1 BTU/s, an increase of 14.4%. However, most of the extra cooling capacity went unused by the evaporator because it was undersized for the higher capacity. This is evident when

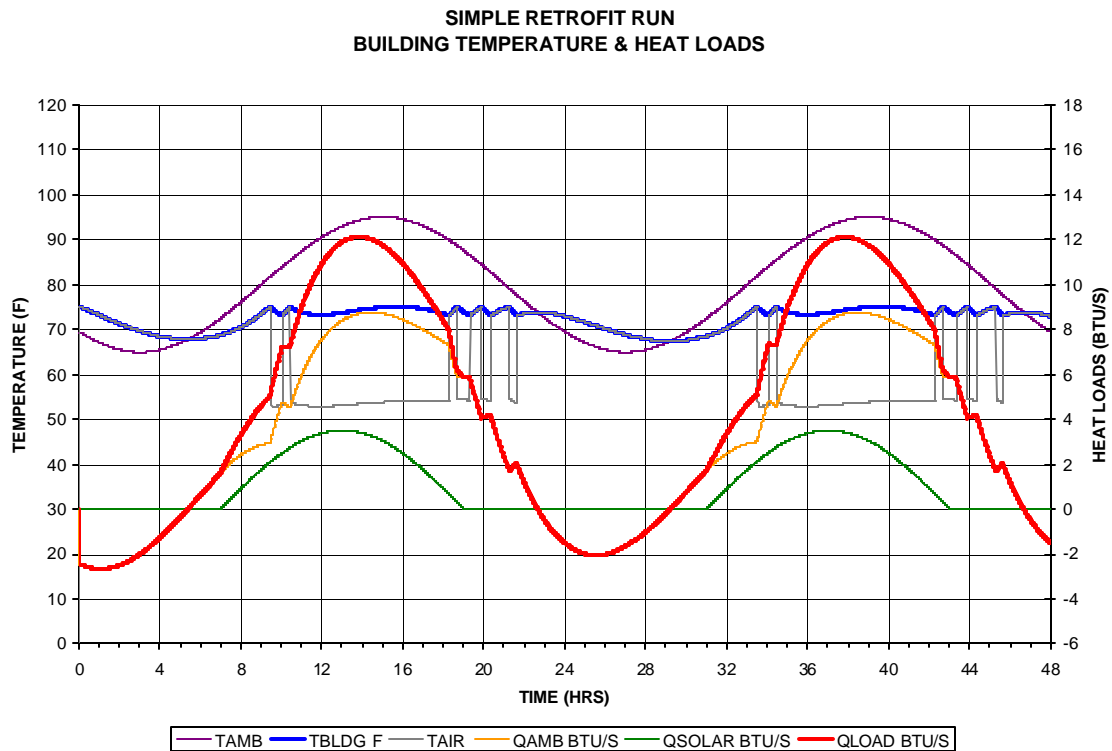


Figure 2-12. Building Temperatures and Heat Load

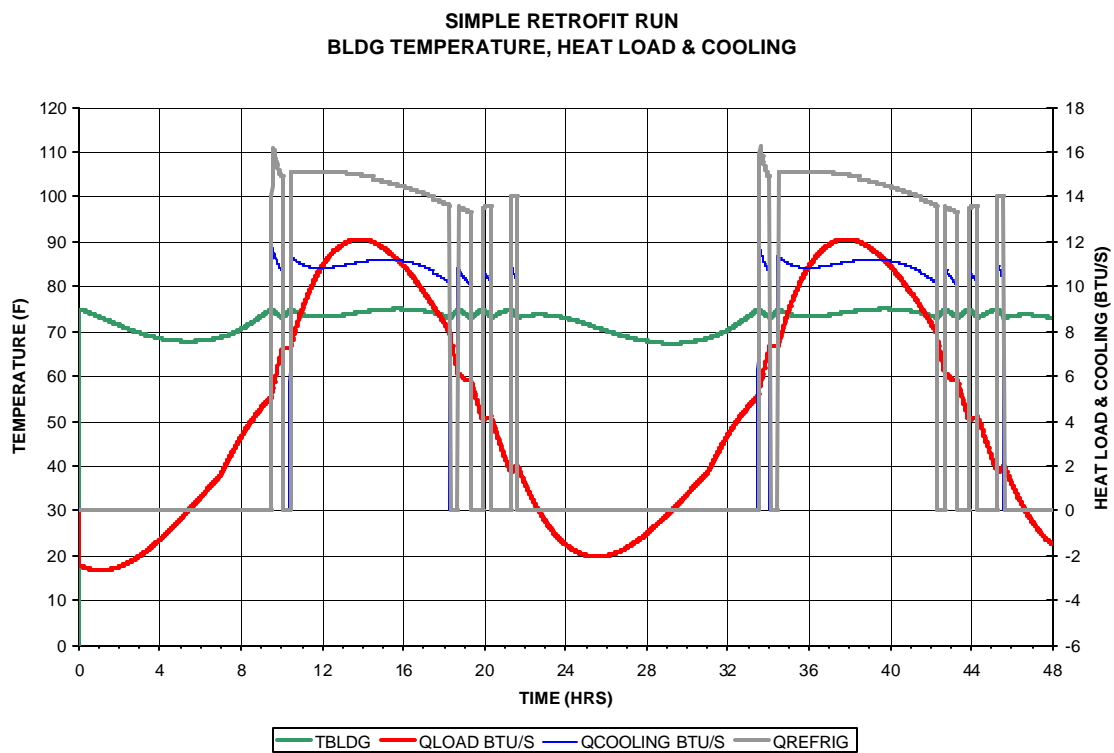


Figure 2-13. Air Conditioner Total and Sensible Cooling

looking at the sensible cooling, which only increased from 10.9 to 11.2 BTU/s, a much smaller percentage increase. This accounts for the small decrease in building temperature.

Where did the extra cooling go? It exited the evaporator as cold liquid, as is shown in Figure 2-14. TEMP5, evaporator inlet and TEMP6, evaporator outlet, are the same for most of the run, indicating that liquid passed through the evaporator. As sized, the evaporator is too small to take advantage of the extra cooling capacity.

A key point illustrating the effect of the Energy Shaver is the difference between TEMP3, the condenser outlet and TEMP4, the Energy Shaver outlet. These temperatures overlapped in the previous cases without the Energy Shaver (ref figures 2-4 and 2-9). Now there is a significant difference due to the cooling provided by the Energy Shaver. TEMP4 initially starts at approximately 70°F because the salt is still cool from the night before. The salt reaches its melting temperature after about 15 minutes of air conditioner operation. From that point, TEMP4 warms as the salt melts and increases the liquid thickness around the heat exchanger. This heat transfer characteristic was taken from the component test results. As can be seen, the temperature warms nearly 15°F during the day. Although this is acceptable performance, it is desirable to minimize the temperature increase in order to maximize the benefit.

Note that there is an abrupt decrease in TEMP6, TEMP7 and TEMP1 near 17:00 hours followed by a gradual increase. This is due primarily to convergence limitations of the Gaspak properties program when the outlet of the evaporator transitions from a liquid/vapor mixture to pure vapor. This has virtually no effect on the results and can be resolved in the future if desired.

Figure 2-15 shows the operating pressures and flow rate. Compare this to figure 2-10. The compressor outlet pressure is the same for both cases, as expected, but the Energy Shaver increases the suction pressure and flow rate. This higher flow rate is a consequence of the lower inlet temperature at the capillary and the higher suction pressure naturally occurs to enable the compressor to match the flow through the capillary.

Figure 2-16 shows the energy consumption and demand of the air conditioner with the Energy Shaver retrofit. The energy consumption does not include the Energy Shaver fan energy. In this instance, there is very little demand and energy savings compared to the baseline case (figure 2-11). The peak demand is reduced by 45 W and 1 kWh/day is saved with the Energy Shaver. The marginal savings result from the system's inability to make use of the extra cooling capacity. The extra cooling capacity is wasted as it passes through the evaporator. This in turn, increases the flow rate and suction pressure, which reduces the enthalpy change during expansion. So, without means of extracting the additional cooling, the system reaches new equilibrium conditions that satisfy the load. These results are for an ideal system. Systems installed in the field may see substantial

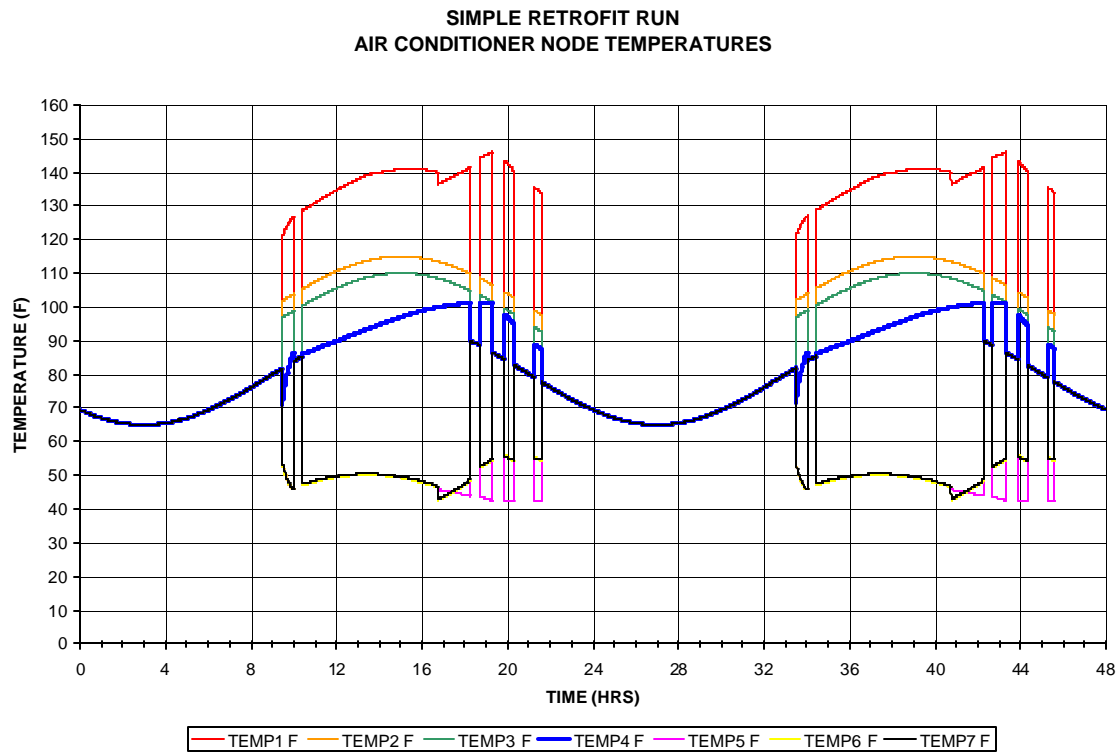


Figure 2-14. Air Conditioner Node Temperatures

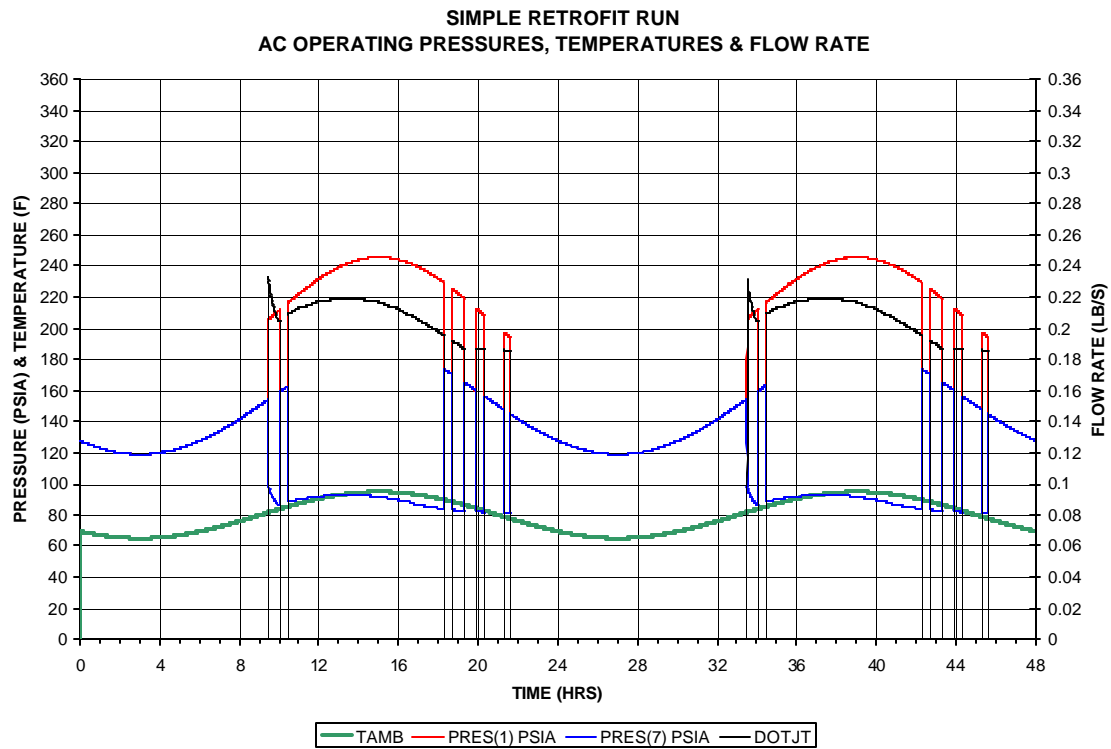


Figure 2-15. Air Conditioner Pressures and Flow Rate

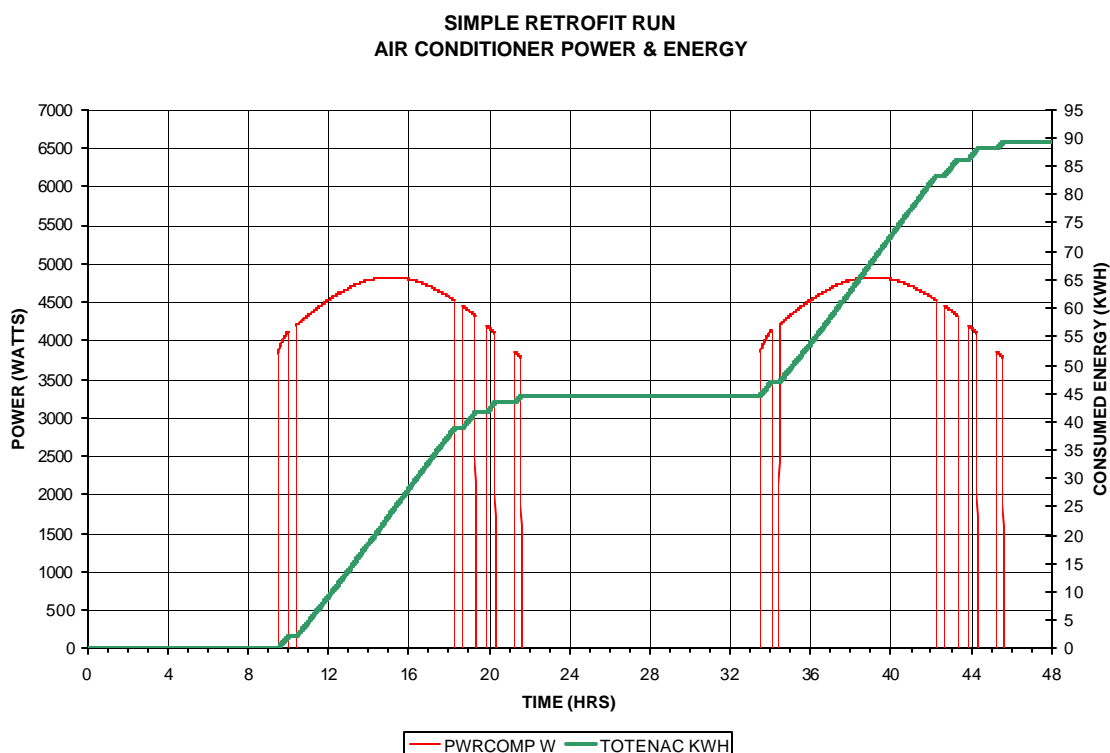


Figure 2-16. Air Conditioner Demand and Energy Consumption

benefit from a simple retrofit for a number of reasons. In particular, if the system is installed on a roof or other hot location, draws hot return air from a high ceiling or has a blower that is oversized for the evaporator. An on-site assessment must be done to determine the overall effectiveness of the Energy Shaver in a simple retrofit application.

The following three graphs show the predicted performance of the Energy Shaver. Figure 2-17 shows the Energy Shaver average temperature (TES) the percent of the salt hydrate that is melted (PCMELT) and the total energy stored in the Energy Shaver (TOTENMES).

The Energy Shaver temperature is set to 70°F for initial conditions. As can be seen, it cools as the night progresses and begins to warm as the sun rises. At this point, it is below the melt temperature of 86°F, so it acts as a solid mass with relatively low heat capacity. It warms rapidly when the air conditioner turns on shortly before 10:00 a.m. until it reaches the melt temperature. It then warms much more slowly, reflecting the high heat of fusion. The average temperature rises throughout the day until the air conditioner turns off at approximately 18:00 hours (6:00 p.m.).

At 19:45 hours, the Energy Shaver thermostat senses that the air temperature is less than 85°F and more than five degrees cooler than the salt and turns on the fan. This is clearly shown in Figure 2-18 and will be discussed shortly. The fan rejects heat to the environment and begins to freeze the salt.

Figure 2-18 shows the fan operation and the consumed energy. The fan is driven by a 1/3 hp motor. The fan logic has two conditions that must be satisfied to turn on the fan: 1) the ambient temperature must be below 85°F, and 2) the ambient temperature must be at least 5°F cooler than the salt. A simple thermostat can be used to implement this logic. As seen in the graph, the fan turns on at approximately 19:25 and remains on until the Energy Shaver cools to 5°F above ambient and then turns off. At this point, the ambient temperature continues to drop and the fan cycles on whenever the 5°F difference is exceeded. This approach ensures that the Energy Shaver is as cool as possible for the next day.

The total energy consumed by the fan is approximately the same as the energy reduction caused by the Energy Shaver, so the net savings was negligible. This result adds confidence that the system model is producing good results because without the ability to extract the extra cooling, the thermodynamic performance should remain the same.

As mentioned previously, actual units in the field may have deficiencies in various parts of the system that allow it to make use of the extra cooling provided by the Energy Shaver. There are also steps that can be taken to ensure the extra cooling is extracted. These include increasing the building blower size or the improving the effectiveness of the evaporator.

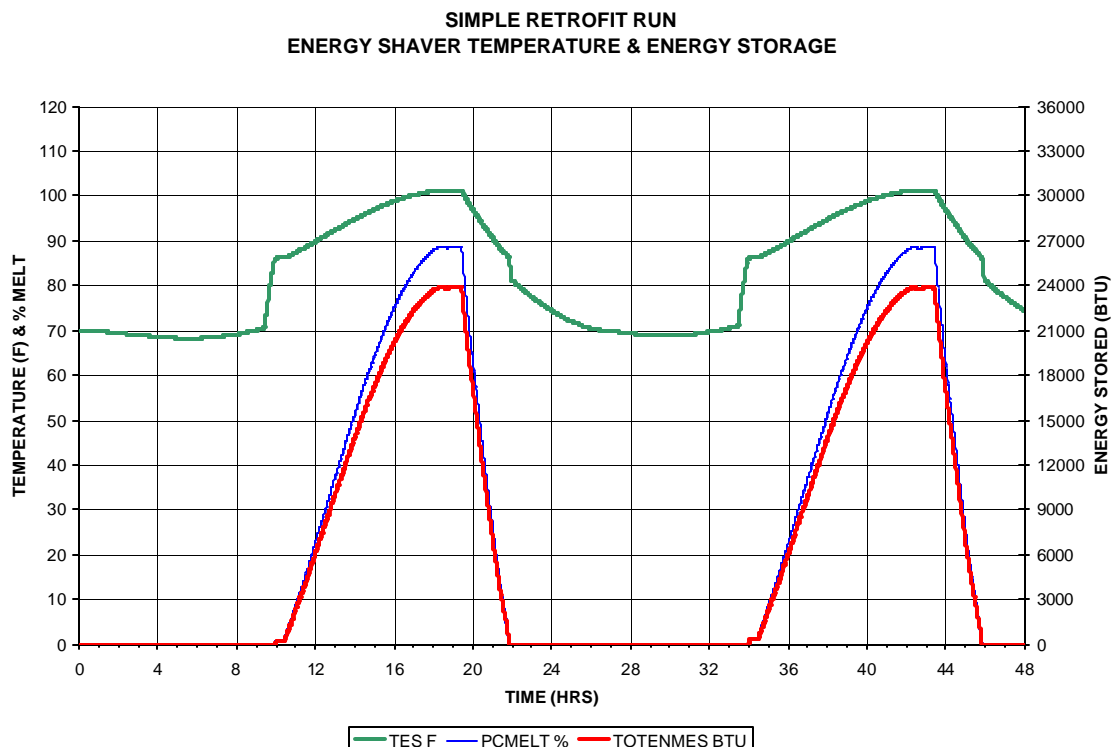


Figure 2-17. Energy Shaver Temperature and Stored Heat

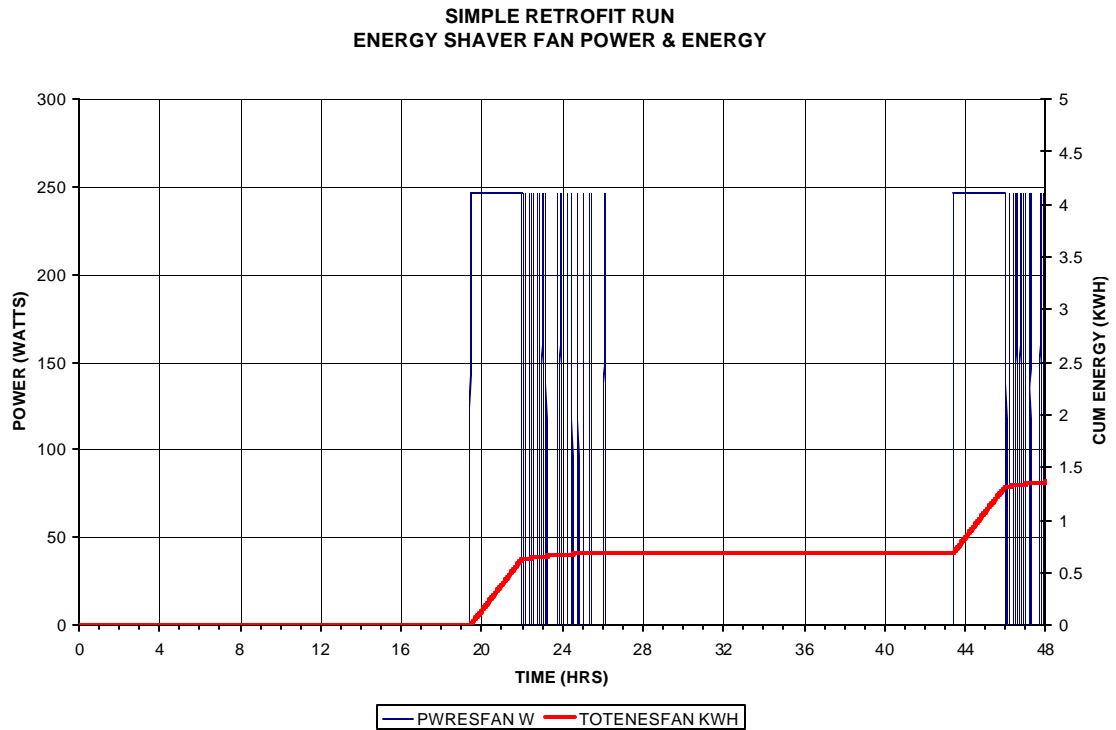


Figure 2-18. Energy Shaver Fan Operation

#### 2.1.3.4 Replacement Case

Another case we investigated was a replacement scenario where the original unit was replaced with a smaller unit augmented with the Energy Shaver. This would offer the most benefit to customers because of the immediate reduction in demand charges in addition to potential energy savings.

For this run, all the environmental conditions and Energy Shaver parameters remained the same as in the baseline and simple retrofit cases. The building blower also remained the same size (for a 4-ton air conditioner). The only change to the model was to reduce the air conditioner size to 3 tons. The results are very positive and are shown below.

Figure 2-19 shows the building data. Comparing the results to those of the baseline case (figure 2-7) reveals very similar performance. The maximum building temperature (TBLDG) is 0.9°F warmer and the supply air (TAIR) is 1.9°F warmer than the baseline case. This is very good considering neither system is meeting the heat load and keeping the building at the thermostat setting of 74°F. Note that the ambient heat load (QAMB), which is proportional to the temperature difference between the ambient and building, is slightly lower for this case because the building temperature is slightly higher.

Figure 2-20 shows the total and sensible cooling capacity. This graphs illustrates why the 3-ton air conditioner with the Energy Shaver can be essentially equivalent to a 4-ton unit under these test conditions. Comparing the total cooling capacity between this case and

the baseline case (figure 2-8) reveals that the 3-ton unit provides less total cooling capacity. The 3-ton unit with Energy Shaver produces 11.5 BTU/s (3.45 tons) of cooling at 12:00 noon whereas the 4-ton unit produces 13.2 BTU/s (3.96 tons), a 14.8% difference. However, what is important for cooling a building is the sensible cooling capacity, i.e., the cooling available to cool the air after removing water from the air by condensation (dehumidification). Comparing the sensible cooling between this case and the baseline case shows much closer performance. The 3-ton unit with the Energy Shaver produces 0.4 BTU/s (0.12 tons) less sensible cooling than the 4-ton unit, only a 3.8% difference. This accounts for the slightly warmer building temperature in this case compared to the baseline case.

The improved performance results from the decreased liquid temperature that the Energy Shaver provides. A lower liquid temperature entering the evaporator has two effects. First, it decreases the liquid's enthalpy so it creates more cooling upon expansion. Second, the lower temperature increases the flow through the capillary. These effects combine to provide significantly more cooling. However, the extra cooling provided by the Energy Shaver does have limitations in its use. The higher flow through the capillary causes the suction pressure to increase (for a constant speed compressor), which increases the operating temperature of the evaporator. Compare these evaporator inlet and outlet temperatures (TEMP5 and TEMP6 respectively) in Figure 2-21 to those of the baseline run, Figure 2-9.

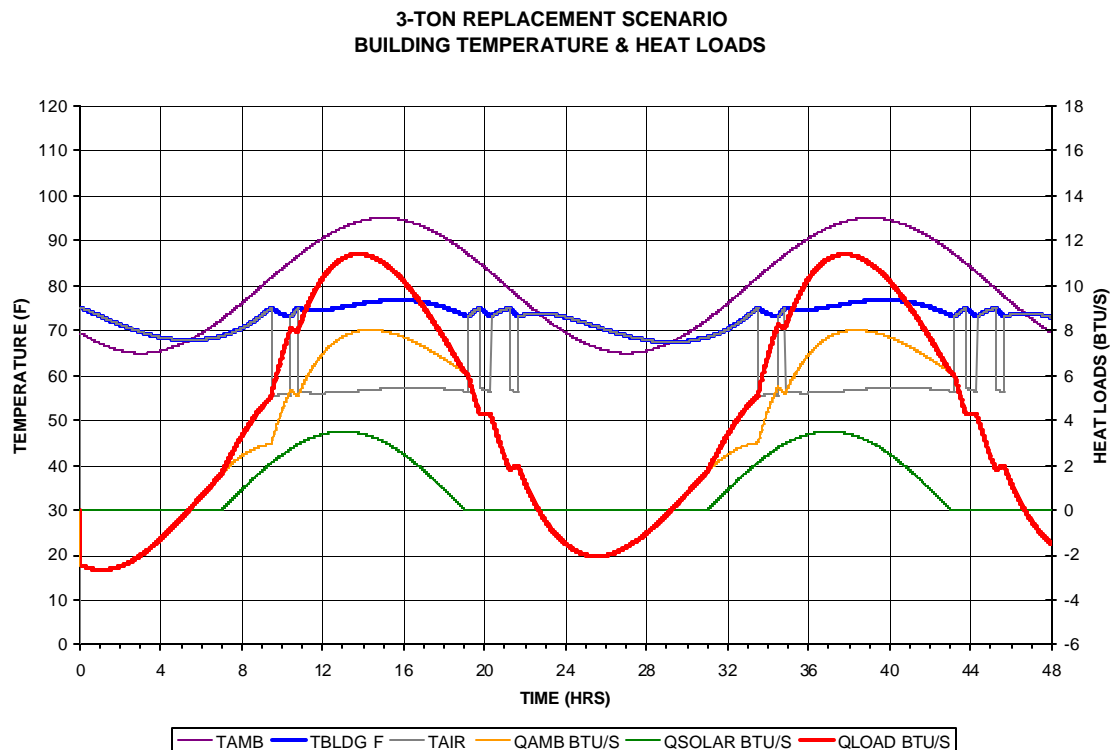


Figure 2-19. Building Temperature and Heat Loads

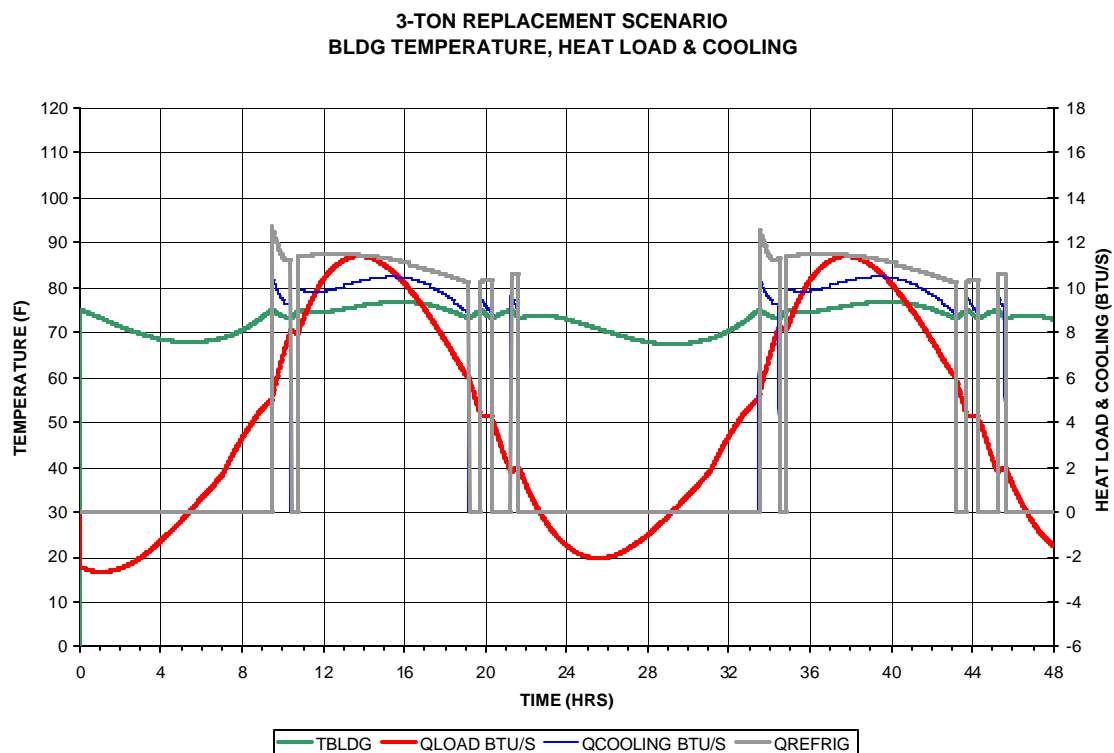


Figure 2-20. Air Conditioner Total and Sensible Cooling

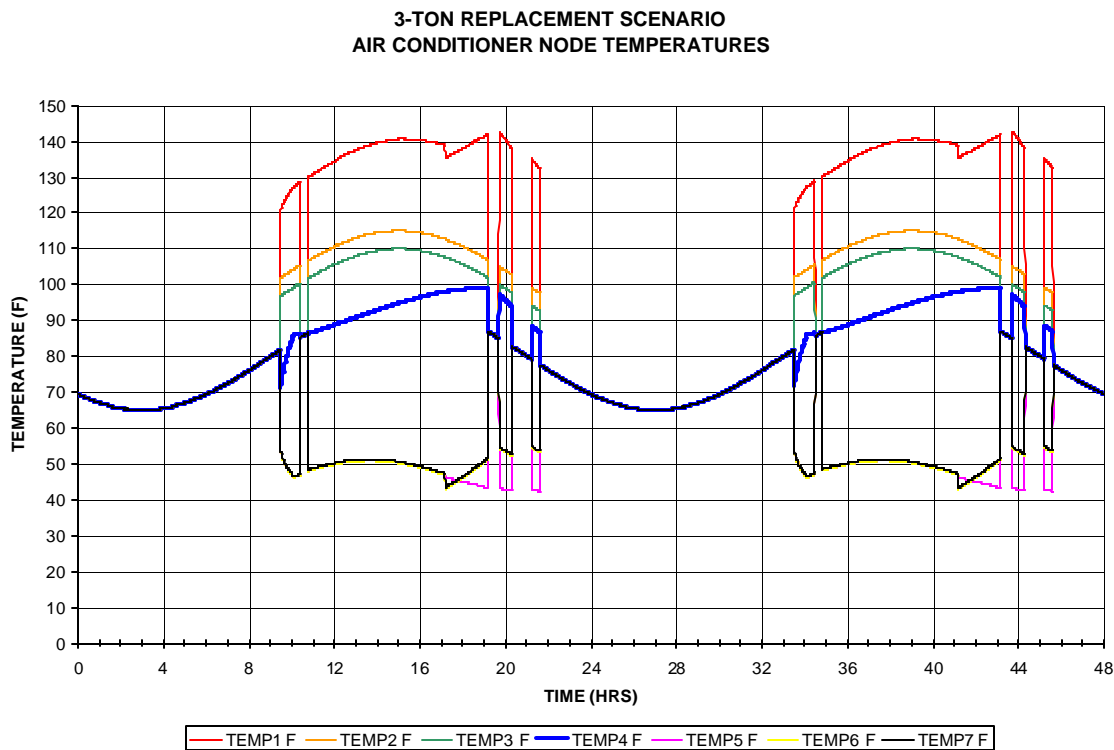


Figure 2-21. Air Conditioner Node Temperatures

In this case, although the evaporator has excess capacity for most of the time, its operating temperature warms to 51°F compared to 45°F in the baseline case. Thus, the Energy Shaver increases the cooling capacity but also raises the temperature at which the cooling is provided.

The impact of the warmer evaporator is greatest when no dehumidification occurs. Figures 2-22 and 2-23 shows the results for a 4-ton unit and a 3-ton unit with the Energy Shaver when no dehumidification occurs. The supply air for the 4-ton unit averages 49°F compared to 54°F for the 3-ton unit with the Energy Shaver. This 6°F difference is significantly larger than the 2°F seen when dehumidification occurred (in the baseline case and the replacement case). Also note that Figures 2-24 and 2-25 show that the total and sensible cooling is now the same in both cases, indicating no dehumidification occurs.

The conclusion drawn from these results is that the Energy Shaver can allow a smaller air conditioner to be used in applications where dehumidification is usually required. Fortunately, most cooling applications require dehumidification. It can also be used when the thermostat setting is set in the upper 70's to allow sufficient cooling to be extracted from the warmer evaporator.

Figure 2-26 shows the operating pressures and flow. Comparing this data to figure 2-10 of the baseline run shows the high pressure is the same for both cases but the flow (DOTJT) is different. This is expected because the baseline case has a 4-ton unit and the replacement case has a 3-ton unit. However, the effect of the lower liquid temperature can be seen by closely comparing the flow rates. The 4-ton unit has a maximum flow rate of 0.196 lb/s, so the expected maximum flow for a 3-ton unit is  $0.196 \times (3/4) = 0.147$  lb/s. But Figure 2-26 shows a maximum flow rate of 0.167 lb/s. The higher flow rate is due to the lower liquid temperature entering the capillary.

Figure 2-27 shows the demand and energy consumption. This graph clearly illustrates the benefits of the Energy Shaver. Compare this data to figure 2-11 of the baseline case. There is a large reduction in demand because the original 4-ton unit that had a 4.8 kW draw was replaced with a 3-ton unit that has a 3.6 kW draw. Thus, *the demand is reduced by 1.2 kW, a 25% reduction*. This represents substantial cost savings for small commercial users because of demand charges. There is also a large reduction in energy consumption. The 4-ton unit consumes 45.7 kWh daily whereas the 3-ton unit consumed 35.0 kWh. When the Energy Shaver fan energy of 0.67 kWh is included, *the Energy Shaver saved 10.7 kWh/day, a 23% savings*. The conclusion drawn from these results is that the Energy Shaver does offer substantial energy and cost savings in a replacement scenario.

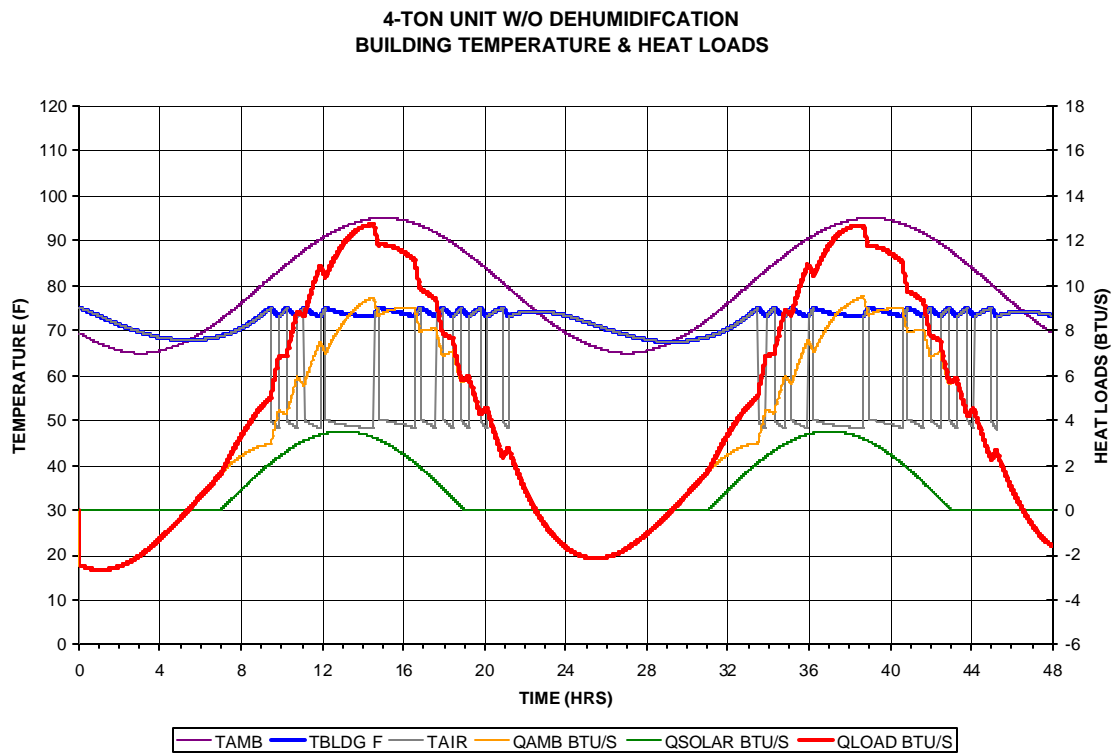


Figure 2-22. Building Temperature and Heat Load (4-Ton Unit)

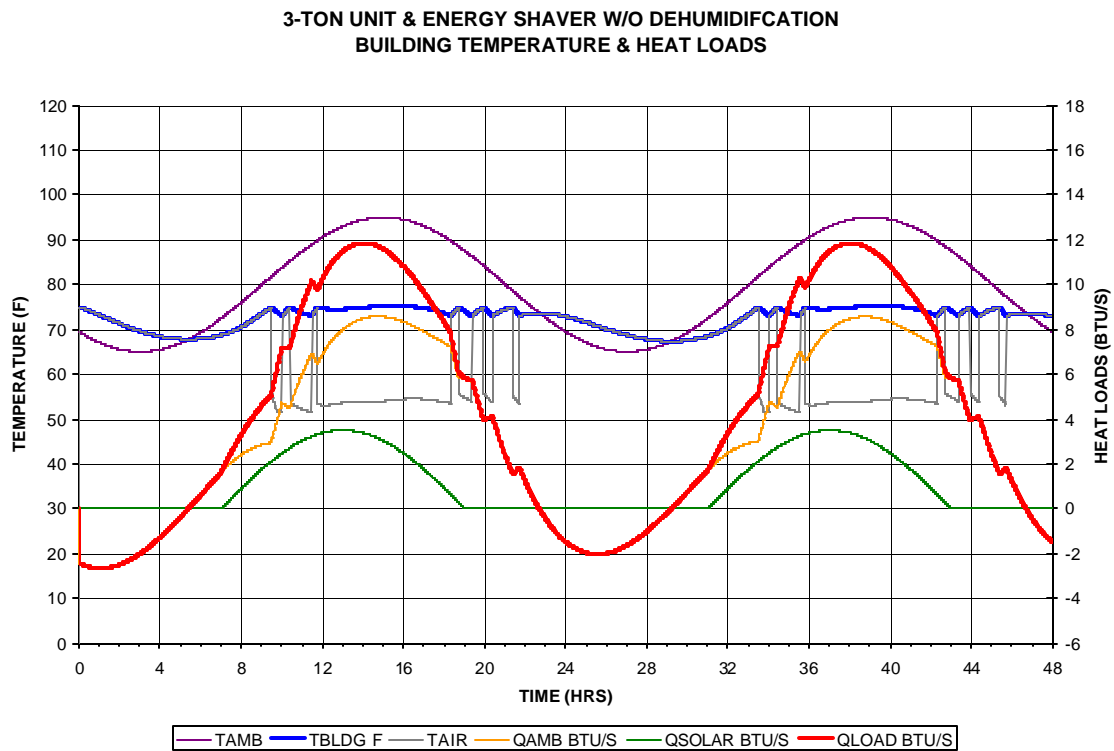


Figure 2-23. Building Temperature and Heat Load (3-Ton Unit)

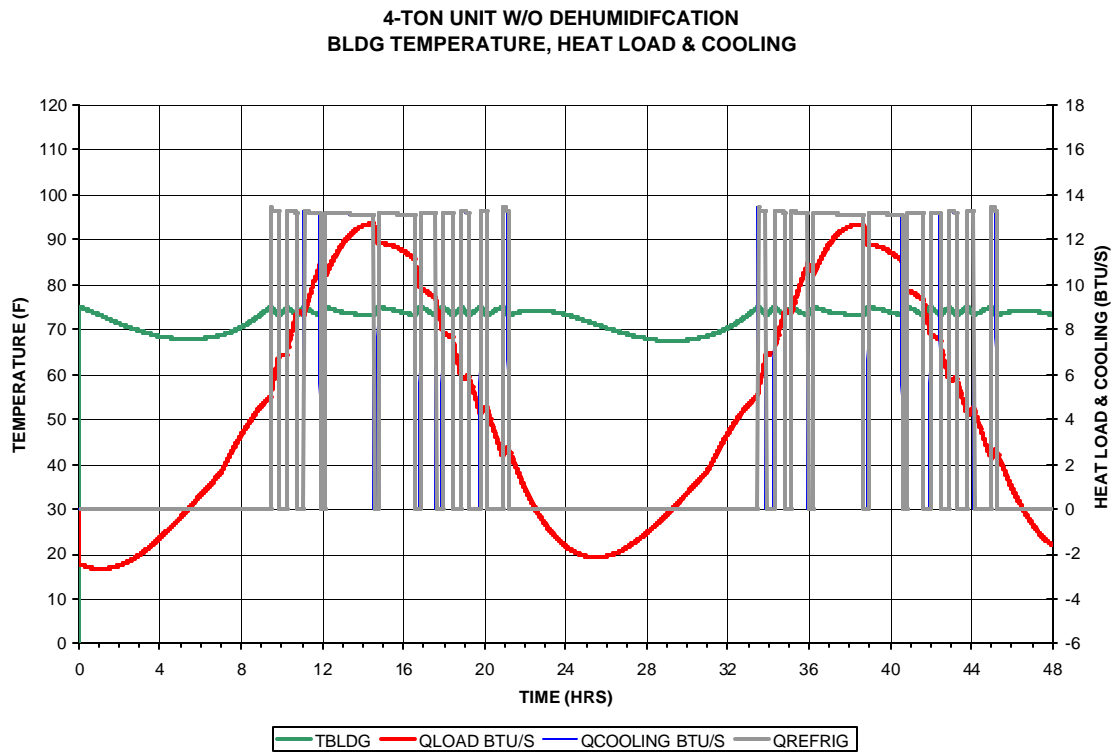


Figure 2-24. Air Conditioner Total and Sensible Cooling (4-Ton Unit)

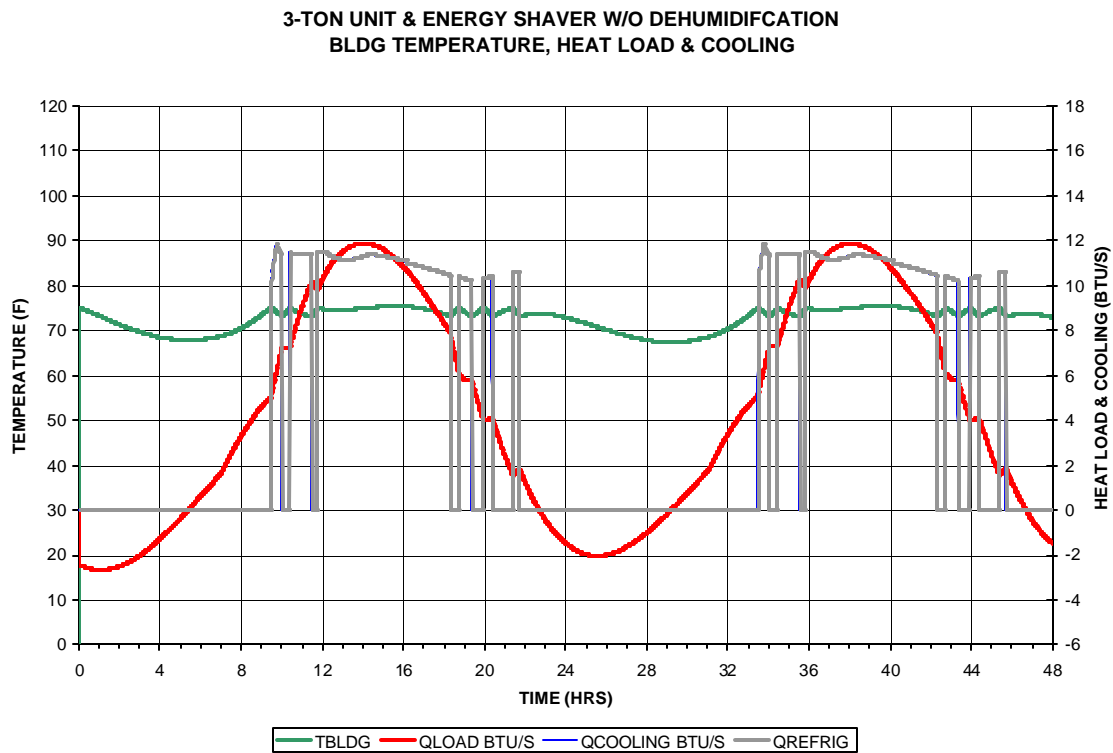


Figure 2-25. Air Conditioner Total and Sensible Cooling (3-Ton Unit)

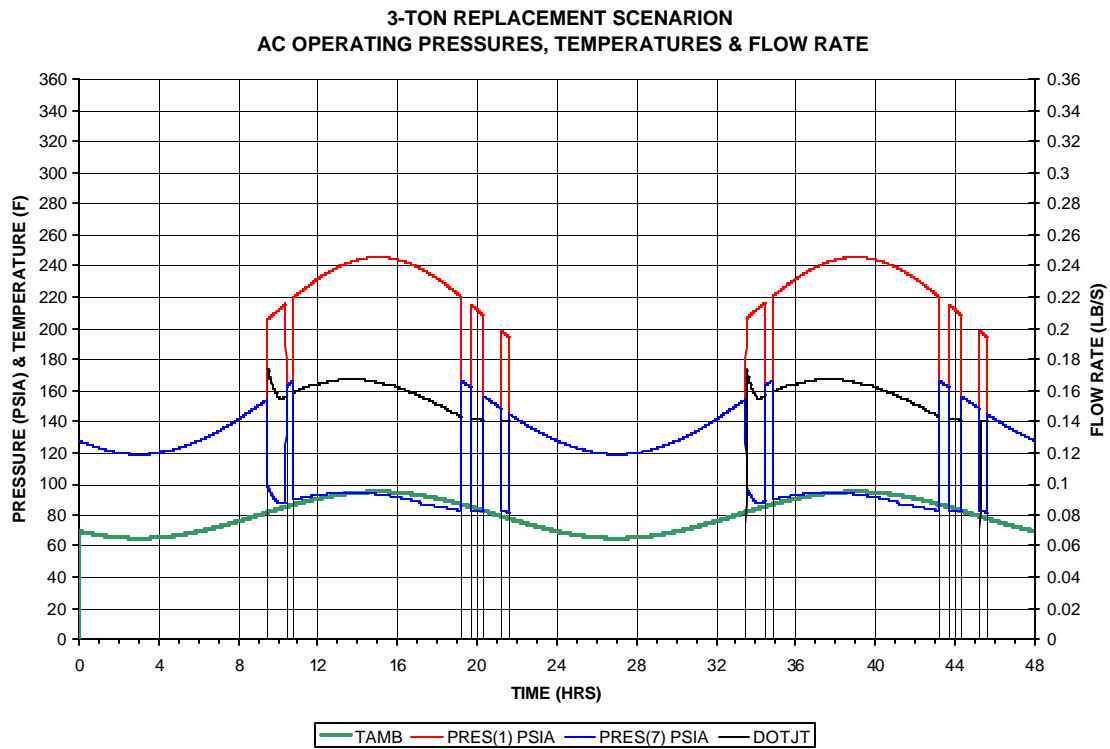


Figure 2-26. Air Conditioner Operating Pressures and Flow

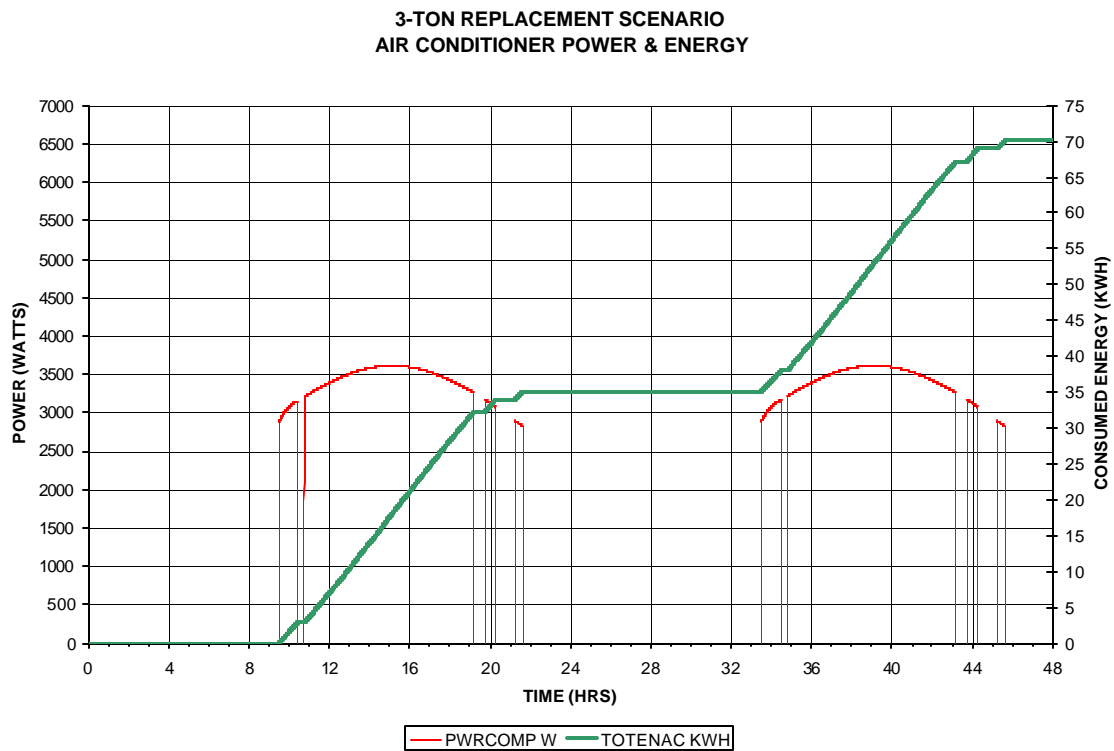


Figure 2-27. Air Conditioner Demand and Energy Consumption

Figure 2-28 shows temperature and stored energy in the Energy Shaver. The results show that a maximum of 77% of the salt hydrate is melted during the day. Therefore, the weight can be reduced from 350 lbs to 270 lbs and still meet the requirements. This amount of salt hydrate can be stored in a 17 inch cube.

Figure 2-29 shows the fan operation and energy consumption. The conclusion from these results is that the fan is properly sized to refreeze the salt before the start of the next day.

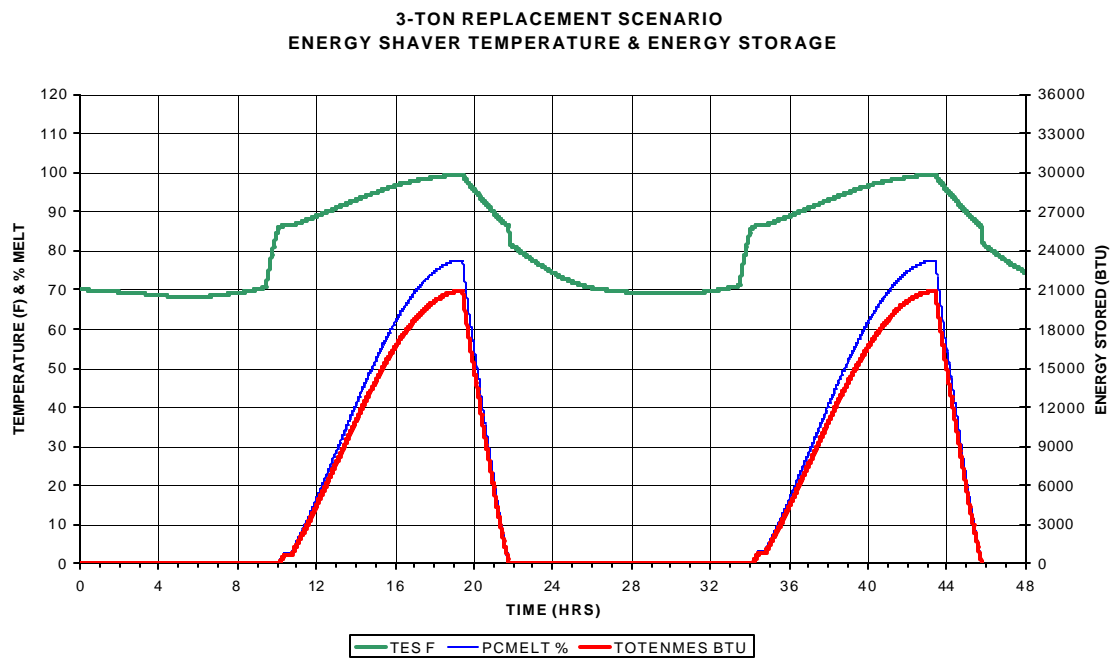


Figure 2-28. Energy Shaver Temperature and Stored Heat

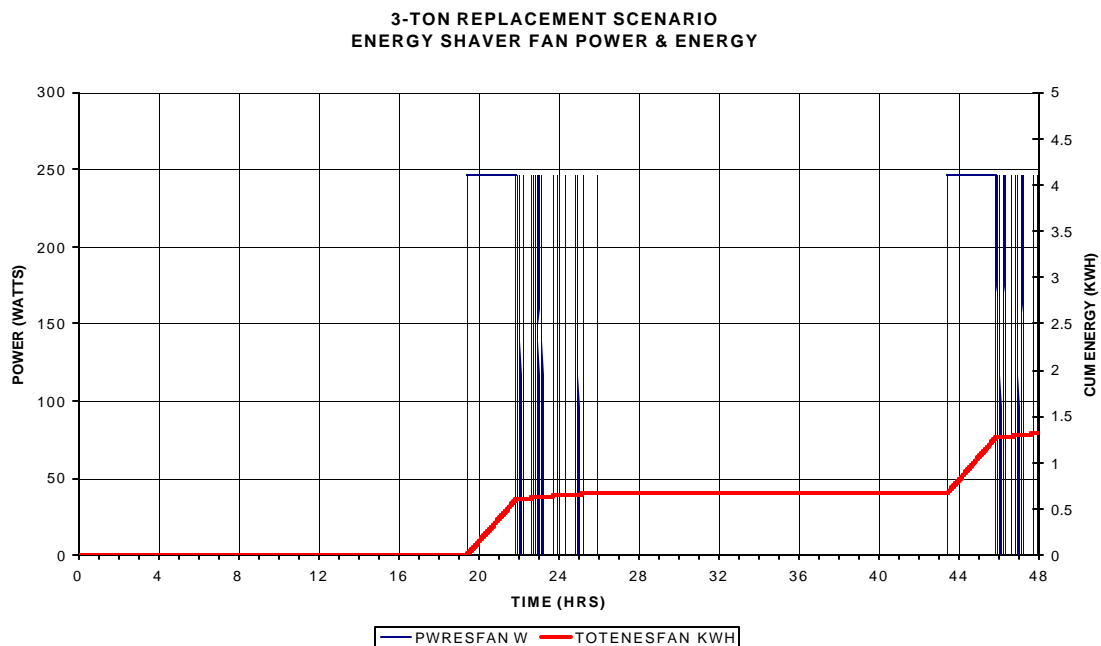


Figure 2-29. Energy Shaver Fan Operation

The following conclusions have been drawn from the modeling results:

- **the Energy Shaver offers substantial benefits to small air conditioning systems in a replacement scenario**
  - the results predict a demand reduction of 25% and an energy savings of 23% when a 4-ton air conditioner is replaced by a 3-ton air conditioner augmented with the Energy Shaver for the test case analyzed
- **modification to the evaporator is necessary in a simple retrofit application to maximize the benefits of the Energy Shaver**
  - a properly balanced system cannot extract the extra cooling the Energy Shaver provides without changes to the evaporator
  - various real-world system deficiencies may be compensated for by the Energy Shaver in a simple retrofit application resulting in improved performance; testing is needed to confirm
- **the Energy Shaver is best suited to applications where dehumidification is usually required**
  - the warmer evaporator temperature performs well when dehumidification is required, but provides less cooling when it is not
- **the melt/freeze cycle can be accomplished with normal ambient temperatures**
  - the fan size combined with the nighttime temperatures freeze the salt

## 2.2 Heat Exchanger Modeling

### 2.2.1 Modeling Objective

The objective of the component models is to develop a set of tools that facilitate thermal design of the Energy Shaver components. These models are used in conjunction with a manufacturability analysis to create a design that can be built for low cost.

There are two models. The Freon-to-hydrate model is used to determine the performance of the Freon heat exchanger for the hydrate melting process. The hydrate-to-air model is used to determine the performance of the air-side heat exchanger for the hydrate freezing process. Both models include pressure loss analysis. The models were created in EXCEL.

### 2.2.2 Model Description

#### 2.2.2.1 Description of the Freon-to-Hydrate Model

Objectives of the Freon-to-hydrate model are to:

- size the Freon-to-hydrate heat exchanger for a range of Freon outlet temperatures and tubing configurations
- calculate the Freon pressure losses in the tubing
- select a practical design

An acceptable solution is one that meets the heat transfer requirements with an additional pressure loss that can be tolerated by the air conditioner compressor and whose cost is minimized.

The baseline heat exchanger consists of a cylindrical coil of standard 5/16" OD refrigeration tubing immersed in the hydrate. We analyzed single, double and triple parallel tube arrangements. The current design does not incorporate heat transfer fins on the coiled tubing in the interest of low cost.

The assumptions and properties used in the Freon-to-hydrate model are:

1. Heat exchange requirements:
  - Freon inlet temperature: 121°F
  - Freon flow rate: 922 lb/hr (5 ton unit)
  - Operating time: 3 hrs
2. Hydrate properties:
  - Melting temperature: 86°F
  - Density of liquid: 1.52 g/cm<sup>3</sup>
  - Heat of fusion: 73.2 Btu/lb
  - Liquid conductivity: 0.0054 W/cm-K
  - Solid conductivity: 0.011 W/cm-K
3. Freon 22 properties @ 300psia, 100°F:
  - Density: 1.14 g/cm<sup>3</sup>
  - Viscosity: 2.20E-03
  - Thermal conductivity: 7.96e-04 W/cm-K
  - Prandtl number: 3.65
  - Specific heat: 1.25 J/g-K
4. Design margin requirements:
  - Hydrate mass: 1.0
  - Freon heat exchanger: 1.2
5. Copper Freon tubing:
  - Outside diameter: 0.794 cm
  - Inside diameter: 0.631 cm
  - Reynold's number: 35568
  - Pressure loss: 0.115 psi/ft of length
6. Freon to tube heat transfer:

Calculation of the Freon to tube heat transfer coefficient is straightforward because the flow rate and tube size are known.

  - Nusselt number: 169
  - Heat transfer coefficient: 0.212 W/cm<sup>2</sup>-K
  - Unit length conductance: 0.420 W/cm-K
7. Heat transfer through tube wall:

The conductance through the copper wall is very high and is, therefore, ignored.
8. Tube through liquid to solid hydrate:

Frozen hydrate surrounds the tube at the start of the melting process. There is a thick layer of liquid hydrate that partially insulates the tube from the 86°F frozen hydrate at the end of the process. As a result, the heat transfer varies greatly between these extremes.

Heat transfer is by liquid conduction and natural convection but these processes cannot be accurately calculated for the baseline configuration. The approach is to calculate an approximate tube to hydrate heat transfer coefficient based on conduction and test for its validity. This coefficient will be adjusted on the basis of test results.

The following procedure was used to arrive at a design:

- A. Establish a tube to hydrate “h” value based on a given tube coil spacing using  $h = k/l$  where  $k$  = the thermal conductivity of the liquid and  $l = 1/4$  of the tube spacing. For a tube spacing of 0.75 inch = 1.91cm,  $h = 0.0054/0.25(1.91) = 0.011$  W/cm<sup>2</sup>-K. The corresponding “u” value is calculated for 1.5 times the outside diameter of the tube.  $u=0.042$  W/cm-K for a unit length of tubing.
- B. Calculate the overall Freon-to-hydrate unit conductance,  $U$ .  $U = 0.038$  W/cm-K.
- C. Calculate the required hydrate mass and tube lengths for a range of Freon outlet temperatures using the unit conductance value “U”.
- D. Select a design from the parametric case study.
- E. Calculate the Freon outlet temperature at the beginning and end of the melting process for this design.
- F. Calculate the container annulus size.

#### 2.2.2.2 Description of the Hydrate-to-Air Model

Objectives of the hydrate-to-air model are to:

- Size the hydrate-to-air heat exchanger for a range of inlet air temperatures and flow rates
- Calculate the air pressure loss
- Select a practical design.

An acceptable solution is one that meets the heat transfer requirements with a pressure loss and airflow that can be obtained from a low cost fan. We analyzed several container wall geometries that serve as the heat exchange surface. The following information gives an overview of the sizing process for the configuration selected from the Freon-to-hydrate model above:

The assumptions and properties used in the hydrate-to-air model are:

1. Heat exchange requirements:
  - Freezing time: 3 hrs
  - Heat released from hydrate: 17427 Btus
  - Air temperature: 72 °F
  - The heat exchanger shall have a design margin of 1.2.
  - Allowable power input to fan: 350 W
  - Fan pressure rise: 1.0 inches of water
  - Fan efficiency: 0.75, minimum
2. Air properties @80°F, 14.7 psia
  - Density: 1.16E-03 g/cm<sup>3</sup>
  - Viscosity: 1.84E-04 g/cm-s

- Thermal conductivity: 2.63E-04 W/cm-K
  - Specific heat: 0.24 Btu/lb-F
  - Prandtl number: 0.707
3. Container wall properties (high density polyethylene)
- Thermal conductivity: 0.003 W/cm-K
  - Thickness: 0.13 cm
4. Container wall to air heat transfer requirements:  
The airflow is split into two streams, one on each side of the annular container.  
The following values apply to one of the air streams.
- Air volumetric flow rate: 18.5 ft<sup>3</sup>/s
  - Air mass flow rate: 1.36 lb/s
  - Air outlet temperature: 74.5°F
  - Log mean temperature difference: 12.7 °F
  - Length of flow path: 48 in.
  - Hydraulic diameter, Dh: 1.1 in.
  - Nusselt number: 69
  - $h = 0.0065 \text{ W/cm}^2\text{-K}$
5. Container wall heat transfer requirements:
- $h = k/L: 0.023 \text{ W/cm}^2\text{-K}$
6. Heat transfer from liquid through solid hydrate to wall:  
Liquid hydrate contacts the entire inside surface at the beginning of the freezing process. Solid forms on this surface and increases in thickness until all liquid has been solidified. As a result, the heat transfer varies greatly between these extremes.
- When solid contacts the wall,  $h$  is very high and is therefore ignored.  
For this case,  $U = 0.0051 \text{ W/cm}^2\text{-K}$
  - When all the liquid has been solidified,  $h$  is based on the annulus thickness.  
 $h = k/L: 0.0058 \text{ W/cm}^2\text{-K}$   
For this case,  $U = 0.0027 \text{ W/cm}^2\text{-K}$

### 2.2.3 Modeling Results

#### 2.2.3.1 Parametric Analysis of Freon-to-Hydrate Heat Exchanger

The following table shows hydrate mass requirements and tubing length results for a design with three tubes in parallel.

Freon temperature parameter:

These values fall in a range that is between hard to easy to achieve.

• Delta T (Freon to solid hydrate) (°F)	4	6	8	<b>10</b>	12
• Freon outlet temperature (°F)	90	92	94	<b>96</b>	98
• Log mean temperature difference (°F)	14.3	16.4	18.3	<b>20.0</b>	21.5

Freon-to-hydrate heat transfer:

• Heat rate for each of 3 tubes (W)	720	675	621	<b>567</b>	513
• Total energy from Freon to hydrate (Btu)	22128	20745	19083	<b>17427</b>	15765
• Mass of hydrate required (lb)	302	283	261	<b>238</b>	215

Freon-to-hydrate heat exchanger:

- |   |      |     |     |            |     |
|---|------|-----|-----|------------|-----|
| • Length of each tube including margin (ft) | 94   | 77  | 63  | <b>53</b>  | 44  |
| • Pressure loss (psi)                       | 10.8 | 8.9 | 7.2 | <b>6.1</b> | 5.1 |

From these results, we selected three parallel tubes, each 53 feet long for the baseline design. All the corresponding baseline parameters are shown in bold.

The Freon outlet temperature at the beginning of the melting process depends only on the unit conductance of the Freon since the 86°F solid is in contact with the tube. Thus, Freon outlet temperature at beginning of melting = 86°F. The Freon outlet temperature at the end of the melting process depends on the conductance of the Freon and the liquid hydrate that is now half the tube spacing thick. Freon outlet temperature at the end of melting = 104°F.

### 2.2.3.2 Hydrate-to-Air Modeling Results

The surface area required for heat transfer is 6306 in<sup>2</sup>. This can be achieved numerous ways. The preferred form for manufacturing is cylindrical. Assuming the following dimensions for a cylindrical annulus leads to a baseline configuration:

Container dimensions (for cylindrical annulus):

- Height: 48 in.
- Height of Freon heat exchanger coil: 43 in.
- Inside diameter: 17.5 in.
- Outside diameter: 20.5 in.

This results in a cylindrical surface area of 2865 in<sup>2</sup>, which is less than the requirement. The solution is to pleat the container walls in the axial direction to increase the surface area while maintaining the overall dimensions.

## 2.3 Thermal Storage Material Evaluation

### 2.3.1 Evaluation Objectives

The objective of this work is to evaluate, adapt and select the best of the solar energy storage phase change materials (PCMs) for use in the Energy Shaver. The Energy Shaver can be made reasonably small and light only if we employ the high latent heat of phase change that occurs at constant temperature.

### 2.3.2 Evaluation Description

The Energy Shaver uses a PCM that alternates between its solid and liquid phases to store and release heat energy. Much research has been done on these materials over the last thirty years for solar energy storage. We have the benefit of this work as a starting point for our PCM investigation. Our PCM has somewhat different requirements than for solar energy uses. For example, our required melting temperature is a few degrees lower. There is now much greater concern for environmental and disposal hazards than in previous years. The Energy Shaver has different economic considerations than those for solar energy storage systems, allowing us to absorb a somewhat higher PCM cost.

Table 2-1 lists PCM requirements we have established for the Energy Shaver. These requirements were derived from our preliminary engineering, economic and safety studies. Materials that meet these requirements give us a good chance to develop a successful product.

Table 2-1. Energy Shaver PCM Requirements

	<b>Requirement</b>	<b>Value</b>	<b>Comments</b>
1	Phase change temperature - °F	82 to 87	
2	Latent heat of fusion – Btu/lb	> 60	
3	Density – lb/ft <sup>3</sup>	> 80	
4	Thermal capacity degradation	< 10% over 2 years	Result of PCM properties and Energy Shaver design
5	Corrosiveness	Low	Must allow low cost construction
6	Fire hazard	None	According to MSDS standards
7	Health effects	Minimal	According to MSDS standards
8	Disposal	landfill safe	
9	Cost - \$/lb	< \$0.20	In large quantities
10	Cost - \$/Btu	0.002	In large quantities
11	Availability – tons/year	> 100,000	For mass production

#### 2.3.1.1 Phase Change Material Candidates and Properties

Few PCMs are available for thermal energy storage in solar systems or the Energy Shaver. Paraffins and hydrates include most of these. Paraffins are ruled out because they are flammable and expensive. There are several hydrates that will meet our thermal and safety requirements but only a few of these are cost effective. Extensive review of literature collected prior to this project identified several useful hydrates. These hydrates are compounds of salts and water where the water bonds to the salt molecules when the temperature drops below the freezing point of the hydrate. This gives the hydrate a large latent heat of fusion that is released when the water/salt solution freezes.

Table 2-2 lists the pertinent properties of these hydrates. These materials meet requirements 5 through 11 of Table 2-1 except for the phase change temperatures of the two sodium hydrates. The desired phase change temperature can be achieved by mixing these two sodium hydrates and by adjusting the water content.

Table 2-2. Properties of Selected Hydrates

Property	Calcium Chloride Hexahydrate	Sodium Sulfate Decahydrate	Disodium Phosphate Dodecahydrate	Mixtures of Sulfate and Phosphate hydrates
Formula	CaCl <sub>2</sub> ·6H <sub>2</sub> O	Na <sub>2</sub> SO <sub>4</sub> ·10H <sub>2</sub> O	Na <sub>2</sub> HPO <sub>4</sub> ·12H <sub>2</sub> O	
Molecular weight	219	322	358	
Phase change temperature - F	85	89	97	77 to 97
Latent heat of fusion – Btu/lb	73	108	114	108 to 114
Density (solid) – lb/ft <sup>3</sup>	107	91	95	91 to 95
Cost - \$/lb (1)	0.07	0.06	0.20	0.06 to 0.20
Cost/Btu - \$/Btu (1)	0.000959	0.000556	0.00175	0.000556 to 0.00175

#### 2.3.2.1 Special Properties and Behavior of Salt Hydrates

Several properties of hydrates limit their use as PCMs or require counteractive measures. These are discussed below.

##### 1. Anhydrous salt settling

This is a problem unique to sodium sulfate. For maximum efficiency we would like to combine the amounts of sodium sulfate and water that totally react to form the hydrate. Unfortunately, not all of the optimum amount of sodium sulfate will dissolve in water. As a result some of the anhydrous salt settles to the bottom of the container and is unused. This problem can be overcome by adding excess water up to the point where the freezing temperature becomes too low. Mixing during freezing is also helpful.

##### 2. Incongruent Melting

The meaning of this term is that when the solid hydrate is melted it tends to separate into its components instead of into a liquid phase that maintains the correct ratio of salt and water throughout. A more dense salt-rich liquid tends to accumulate at the bottom of the container and a water-rich salt solution rises to the top. Over repeated freezing and melting cycles, less and less of the salt and water can come together and react to form a hydrate with the desired melting temperature. Some of the solid cannot be melted; and, some of the liquid cannot be frozen. The effect is a gradual loss of latent heat capacity. The degree of incongruent melting varies among hydrates. Some hydrates do not exhibit incongruent melting but the only ones we found are either too expensive or do not have acceptable thermal properties. One or more of the following methods must be used to overcome incongruent melting:

a. Mixing

The most effective method of correcting for incongruent melting is to physically mix the water-rich and salt-rich parts of the melt before each freezing cycle. When thoroughly remixed, the bulk latent heat returns to the “new” value. Mixing can be done by mechanically stirring or by pumping air or an immiscible fluid through the melt. All mixing approaches increases the overall cost.

b. Suspension

The salt and water can be suspended in a clay or gel. This way, these components are always kept in proximity and can react repeatably without the need for stirring. These measures also add to cost.

c. Shallow container geometry

Short vertical dimensions of the container minimize separation of salt and water and minimize the loss of latent heat. This method creates difficulties with the necessary heat transfer processes and adds to cost.

3. Supercooling and nucleation

We are used to water. Water always freezes very near 32°F unless it is very highly purified. Unlike water, the salt hydrates have a marked tendency to supercool before freezing is initiated. Supercooling can be as much as 20°F. The bad effect of supercooling in the Energy Shaver is that freezing might not be initiated within the temperature range of the ambient air-cooling medium.

Adding a small amount of a nucleating agent can nearly eliminate supercooling. This agent is a solid additive in the melt that provides an easy place for crystals to start growing. A partially effective method of correcting supercooling is to use salt that is not too pure. Contaminants in the salt act as nucleators. Impure salt is also less expensive. A nucleating agent works best when its microscopic physical form is similar to (isomorphic with) the desired hydrate crystals. Borax works well with sodium based hydrates. Strontium chloride works with Calcium chloride. Nucleators are used in small quantities and have little effect on cost.

4. Crystal growth rate

Some hydrates tend to grow very large crystals at a slow rate. The bad effect of large crystals is that complete freezing can be difficult to achieve in the Energy Shaver within the available time. Small crystals are more desirable because they present a much greater surface area for additional crystal growth. The total freezing time is thereby minimized. Additives, called crystal habit modifiers, are used to promote small crystal growth. The cost of crystal habit modifiers is minimal.

5. Formation of undesired hydrates

Calcium chloride, in particular, tends to form a small amount of tetrahydrate in addition to the desired hexahydrate. The tetrahydrate is not useful as a PCM and gradually reduces latent heat capacity. Additives can minimize the formation of the undesired hydrates. The cost of these additives is minimal.

## 3 Project Testing

### 3.1 Heat Exchanger Testing

#### 3.1.1 Heat Exchanger Test Objectives

The test objectives were to:

- Verify the heat exchanger performance predictions for the salt melting process.
- Identify limitations and potential improvements for the Freon-to-hydrate model.

#### 3.1.2 Bench Test Description

The bench test was designed to use water at a flow rate of one gal per hour as a substitute for Freon. Tube spacing, container wall spacing and the hydrate were the same as in the full size Energy Shaver. We wanted the heat flux per degree of temperature difference to be the same for the full size Energy Shaver and the bench test to maintain equivalent heat transfer conditions. This condition requires a scaling factor. The scaling factor calculated from the full size Energy Shaver is:

$$SF = m \text{ Cp}/A$$

where  $m$  is the mass flow of the Freon,  $C_p$  is the Freon specific heat and  $A$  is the tube outside area.  $SF = 0.012 \text{ J/g Cm}^2\text{-K}$ .

The equation for  $SF$  is then solved for the bench test tube area, knowing the mass flow and specific heat of water. This calculation results in a bench test heat exchanger tube six feet long.

A schematic and photo of the bench test setup are shown in Figures 3-1 and 3-2. A submersible water pump sits in the bottom of the bucket and pumps water through the six-foot copper heat exchanger coil immersed in the salt hydrate. The bypass valve controls the flow rate through the tubing to 1 gph. An in-line flow meter measures the flow and displays it on the small meter on top of the thermocouple data recorder. Water was circulated through the heat exchanger after being heated to a controlled temperature close to the normal Freon inlet temperature of 121°F. Heat exchanger inlet and outlet temperatures were recorded with thermocouples attached to the tubing. A probe was immersed in the salt hydrate to measure its bulk temperature. A thermocouple was also used to measure the ambient temperature.

#### 3.1.3 Heat Exchanger Test Results

Typical test results are shown in Figure 3-3. In this test, all of the hydrate was solid and subcooled to 77°F at the beginning of the test. The water was heated to a target temperature of 120°F. The water temperature was controlled by manually adjusting a power knob on the hot plate. The test was conducted for 180 minutes. The outlet temperature rose by 22°F at the end of the test when the hydrate was completely melted, as shown in Figure 3-4. The temperature sensor immersed in the hydrate showed a similar temperature rise throughout the test. The hydrate temperature sensor was in warm

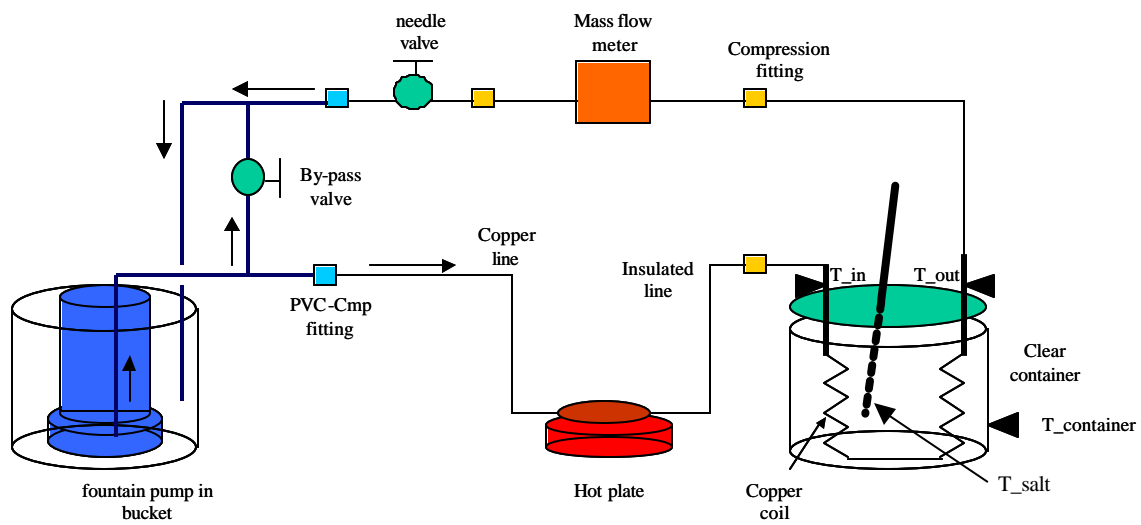


Figure 3-1. Schematic of Bench Test Setup

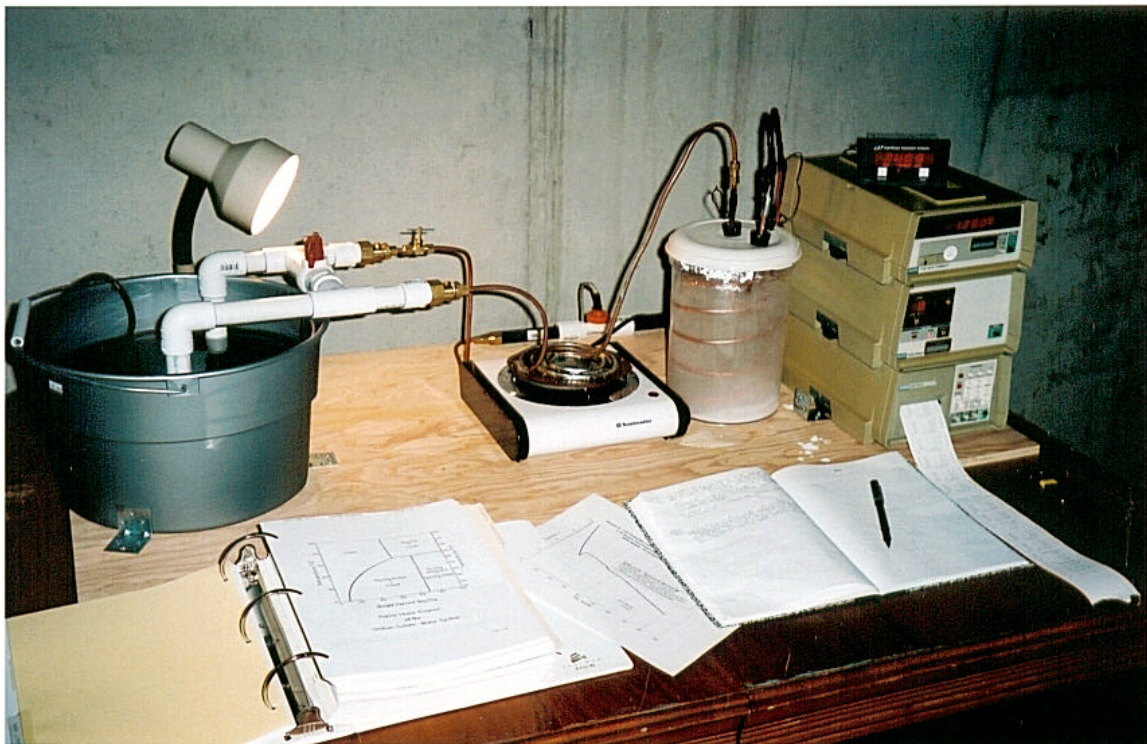


Figure 3-2. Photo of Bench Test Setup

### Heat Exchanger Test Results

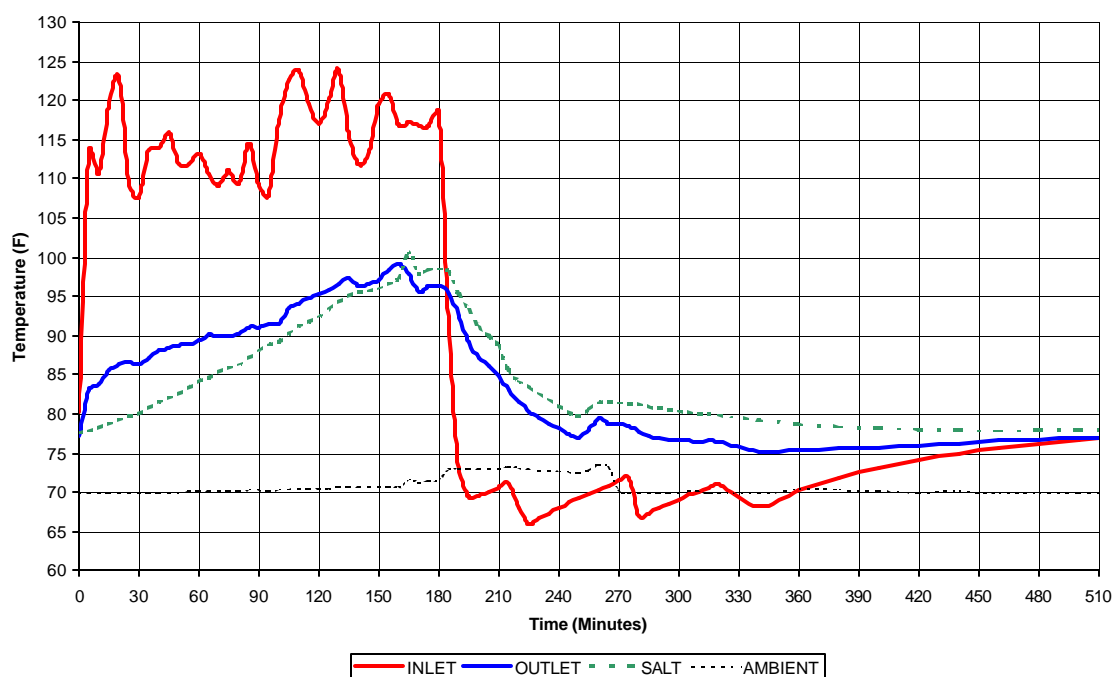


Figure 3-3. Bench Test Results of Freon-to-Salt Heat Exchanger

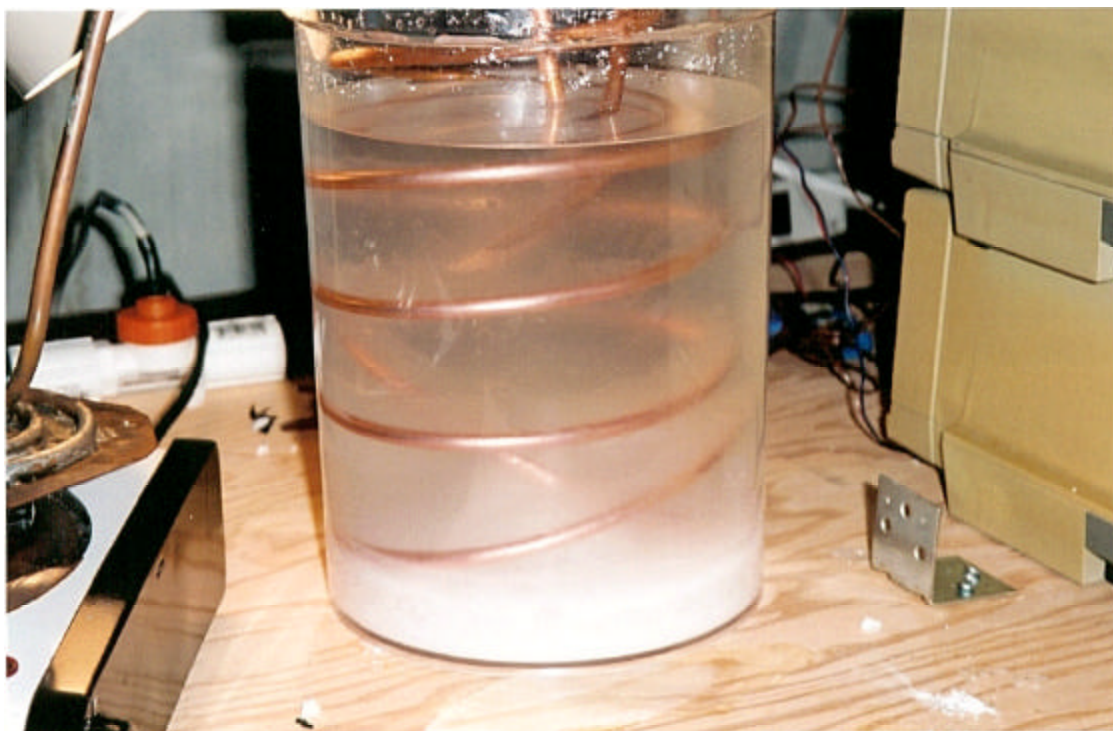


Figure 3-4. Photo Of Fully Melted Salt Hydrate At End Of Test

liquid for most of the test. Previous measurements showed that despite the warm liquid temperature, the remaining solid hydrate stayed at 86°F.

The salt hydrate was frozen by turning off the hot plate and putting ice into the bucket to lower the water temperature. Cold water was then circulated through the heat exchanger. The freeze cycle progressed as expected. Slight supercooling was observed at about 250 minutes.

### **Correlation of Test Data With The Freon-to-Hydrate Model and Discussion**

The outlet water was cooled to the hydrate temperature at the beginning of the melting cycles. The model predicted this result. Strong agreement was expected for this starting condition because the poor thermal conductance of liquid hydrate does not enter into the heat transfer process.

The outlet water temperature rose 22°F by the end of the test and nearly equaled the hydrate temperature. The model predicted a rise of 18°F in three hours. Thus, in its present form, the model under-predicts the temperature rise for the bench test.

This is why component testing is so valuable, particularly when trying to project performance of a complex process such as this. Correlating the model to actual test results is the only way to gain confidence in future designs. The conclusion drawn from this effort is that additional heat transfer area (longer tubes or extended surfaces) is necessary to meet the heat transfer requirements.

These results were integrated into the system model before producing the results reported in earlier sections.

## **3.2 PCM Testing**

### **3.2.1 PCM Test Objectives**

Existing literature provides most of the information needed for PCM selection. The objectives of this new work are to:

- Discover any PCM implementation problems for the Energy Shaver
- Develop corrective action
- Select a single PCM

The test scope addresses items that were not adequately discussed in the literature. The tests are designed to provide an understanding of the special properties so that an Energy Shaver PCM can be selected. This is a multi-dimensional problem in that the special properties combine in various ways. For example, it is often difficult to determine if the observed melting temperature is due to the bulk mixture ratio or is altered by the special properties.

Tests were performed to answer the questions below.

1. Initial mixing and hydrate preparation:
  - How do we mix the dry salt and water to avoid caking and settling and to get a good solution?
  - Is dry salt granule size important?
  - What water temperature is needed?
  - Is the release of heat of solution a problem?
2. Supercooling, nucleation and additives:
  - How do we prevent the temperature from dipping too far below the theoretical freezing temperature at the start of freezing?
  - What and how much additive do we need to promote nucleation and freezing at the right temperature?
3. Crystallization rate, crystal size and additives
  - Is crystal size important?
  - What and how much additive do we need to control crystal growth?
4. Adjustment of melting temperature by hydrate mixture ratio and water
  - What mixture ratio of hydrates gives us the desired 82 to 87K°F freezing temperature?
  - Should we add excess water?
5. Cyclic repeatability
  - Is mixing necessary to avoid degradation due to incongruent melting behavior or settling?
6. New findings
  - Any surprises not evident in the literature?

We did not attempt to determine any basic hydrate properties such as latent heat, density, or thermal conductivity. This information is readily available from several sources.

### **3.2.2 PCM Test Description**

PCM testing consisted of preparing samples of various salt hydrates and then running freezing and melting tests.

#### **3.2.2.1 Initial Mixing**

Initial mixing questions were answered in the course of preparing samples for freezing and melting tests. We purchased readily available granular salts.

Calcium chloride comes as a dihydrate that contains 20 percent water that must be accounted for in hexahydrate preparation. The granules easily dissolve in cold tap water because a large heat of solution is released, heating the liquid to at least 140°F. No salt settled out of the solution at the hydrate freezing temperature. Many tons of solution would be made in mass production. Rejecting the large amount of released heat would be a significant production problem.

Sodium sulfate comes in an anhydrous granular form. This salt dissolves in warm water and only a small heat of solution was observed. Five to ten percent of the desired salt

will not dissolve at the hydrate freezing temperature and settles to the bottom of the container.

Disodium phosphate also comes in an anhydrous granular form. This salt dissolves in warm water and only a small heat of solution was observed. This material is more soluble than sodium sulfate and no settling was observed at the hydrate freezing temperature.

#### 3.2.2.2 Calcium Chloride Hexahydrate Test

Calcium chloride hexahydrate has been studied extensively. We have previously run tests on this material with partial success. Tetrahydrate formation and/or incongruent melting were present and caused serious degradation. Degradation was apparent as less and less of the material froze on repeated cycles. The above reference suggested that excess chloride ions in the raw salt lead to the formation of tetrahydrate. The reference suggested adding a small amount of Calcium Hydroxide (hydrated lime) to get chloride ions.

A sample consisting of 48% Calcium chloride, 52% water and an added 0.2% Calcium hydroxide was prepared. This sample was subjected to 10 repeated freezing and thawing cycles. Immediately, on the second cycle, excess water appeared and increased with cycling. We are not able to determine if the degradation was due to tetrahydrate formation or incongruent melting.

Since the tetrahydrate problem overlays incongruent melting it is difficult to analyze and cure without special equipment. Therefore, we decided to suspend testing on the calcium chloride hydrate and go on to the other hydrates in the interest of cost and schedule. Calcium chloride hexahydrate is still attractive because it is inexpensive. We plan to resume testing in the future when more thorough chemical analysis is possible.

#### 3.2.2.3 Single Hydrate Tests

The sodium sulfate and disodium phosphate hydrates both have theoretical phase change temperatures higher than required. These two hydrates must be mixed to get the desired phase change temperature of 82 to 87°F. We first ran tests on the individual hydrates to assess general behavior and to determine the need for modifications.

Testing consisted of measuring the freezing points of various samples. The special properties were observed for each sample. Table 3-1 summarizes the results.

### 3.2.3 PCM Test Results

#### 3.2.3.1 Discussion of the Single Hydrate Test Results

Sample 9, made with a pure grade of disodium phosphate exhibited a 21°F supercooling effect shown in Figure 3-5. Freezing then started abruptly and temperature increased to 97°F as expected. The supercooling effects were inconsistent for the other disodium phosphate samples. Slight movements could sometimes abruptly start the freezing

process. Chance nucleation on contaminants or container walls appears to be random. Incongruent melting was evident as indicated by both the gradual increase in free water at the end of successive freezing cycles and the decrease in freezing temperature.

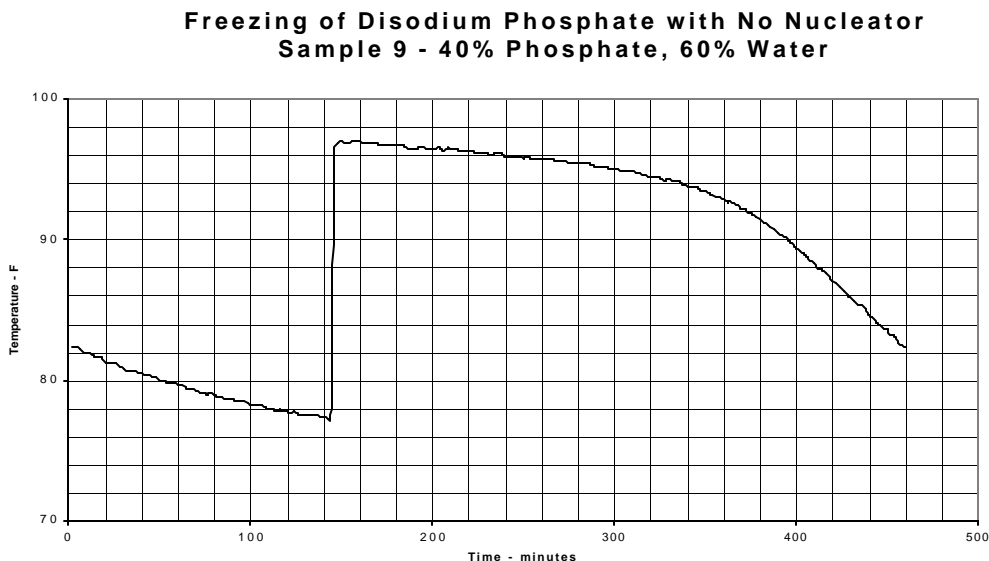


Figure 3-5. Test Results for Disodium Phosphate Without Nucleator

The pure sodium sulfate, Sample 10, exhibited a lower than expected freezing temperature of 77°F. This is probably due to the fact that the required amount of anhydrous salt could not be dissolved in the initial sample preparation.

Conclusions from the single hydrate tests are as follows:

- Nucleating agent must be added to stabilize and minimize supercooling of the disodium phosphate hydrate.
- Mixing or other corrective measures will be needed to maintain long-term thermal performance through of the disodium phosphate hydrate with cycling.
- The thermal capacity of the sodium sulfate hydrate is reduced about 10% by insoluble salt settling.

### 3.2.3.2 Disodium Phosphate/Sodium Sulfate Mixed Hydrate Tests

These two hydrates must be mixed to get the desired phase change temperature of 82 to 87°F. In addition, mixing hydrates allows us to reduce the required percentage of sodium sulfate. This, in turn, minimizes anhydrous sodium sulfate settling. Limited data is available on the freezing temperatures of various mixtures. The data indicate that freezing temperatures well below the freezing points of either hydrate can be obtained as expected for mixtures. Except for sample 5, all mixture ratios were chosen such that theoretically all of the salt and water would react to form the hydrate.

Testing consisted of measuring the freezing points of the various mixtures. The results are shown in Table 3-2.

**Table 3-1. Freezing Tests of Single Hydrate Samples\***

#	Composition %Phosphate/ %Sulfate/ %Water	Salt Source/ Purity	Additives	Sample Size Oz.	Freezing Point / Supercooling F	Freezing Cycles	Notes
9	40/0/60	Mallinkrodt Baker/ 99.5%	none	5	97/21	16	Freezing point after 16 cycles was 88F. No free water remained after last cycle.
13	35/0/65	Mallinkrodt Baker/ 99.5%	none	5.7	83/14	6	Freezing point after 6 cycles was 80F. Free water increased with cycling.
14	35/0/65	Mallinkrodt Baker/ 99.5%	0.1% Colloidal silica	5.7	96/26	1	This amount of colloidal silica did not reduce supercooling. No free water remained when frozen.
15	40/0/60	Mallinkrodt Baker/ 99.5%	0.5% Colloidal silica	5	95/2	3	0.5% colloidal silica appears to reduce supercooling. 5% free water remained after last cycle.
16	40/0/60	Mallinkrodt Baker/ 99.5%	1% Borax	5	96/21	3	This amount of Borax (Sodium Tetraborate) did not reduce supercooling. 5% free water remained after last cycle.
17	40/0/60	Lidochem/ food grade	none	5	97/21	1	The more pure food grade does not appear to be self-nucleating. 4% free water.
18	40/0/60	Lidochem/ FCC grade	none	5	95/3	1	The less pure FCC grade appears to be self- nucleating. 8% free water.
19	40/0/60	Lidochem/ FCC grade	none	10	94/20	2	Larger sample of FCC grade. Trace free water.
10	0/43.5/56.5	No. Amer. Chem. 99%	none	4.6	77/3	1	8% anhydrous salt would not dissolve and settled. About 10% free water.

\*No agitation or mixing between cycles

**Table 3-2. Freezing Tests of Disodium Phosphate/Sodium Sulfate Mixtures**

#	Composition %Phosphate/ %Sulfate/ %Water	Additives	Sample Size Oz.	Freezing Point/ Supercooling F	Freezing Cycles	Notes
4	15/27/58	0.75% Borax	6.7	77/3	2	Slight salt settling. <5% free water remained when frozen.
5	18/19/63	0.9% Borax	11.1	72/2.5	1	22% free water remained when frozen. All froze after 7 days.
6	12.5/27.5/60	0.6% Borax	16	79/7	1	Slight salt settling. <5% free water remained when frozen.
7	21/19/60	1% Borax	9.5	79.5/2	1	More Borax reduced supercooling. More free water than # 6.
8	21/19/60	5% Borax	9.5	75/1	1	Much more Borax. Much more free water than #7.
11	35.5/5/59.5	none	5.6	89/17	4	Large supercooling.
12	31/10/59	none	6.5	72/>25	1	Did not nucleate and freeze.
20	10/32.2/57.5	3% Borax	15.4	80/2	2	Mixed in hot water. Trace water when frozen.
21	10/32.2/57.5	3% Borax	15.6	81/3	1	Mixed in warm water. Trace water when frozen.
22	10/32.5/57.5	3% Borax	89.6	82/4	2 + air	Slight salt settling. Free water 3% on first cycle but water increased in second cycle. Forced air mixing tube froze.
23	32/8/60	3% Borax	85.9	93/4	1 + air	10% free water. Forced air mixing tube froze.
24	30.6/12.2/57.2	3% Borax	89.9	101/2	1 + air	5% free water. Forced air mixing tube froze.
25	28.8/11.6/59.5	3% Borax	94.9	96/1	2 + air, 1+ oil	5% free water. Free water increased with cycles. Forced air mixing tube froze. Oil circulation tube froze.
26	30/13/57	3% Borax	90.3	97/0	1 + oil	5% free water. Oil circulation tube froze.
27	35/8/57	3% Borax	90.3	96/0	3 + auger	No free water after first cycle, increased with cycles. Auger did not freeze.
28	5/35/60	3% Borax	85.9	83/3	3 + auger	5% Salt settled. 8% free water after first cycle, did not increase with cycles. Auger did not freeze.

Samples 22 through 28 also contained 0.1% sodium hexametaphosphate to promote growth of small crystals that increase freezing efficiency.

### 3.2.3.3 Discussion of the Mixed Hydrate Test Results

This series of tests was primarily directed at finding a Phosphate/sulfate hydrate mixture with a freezing temperature of 82 to 87°F. This was done by making educated guesses from a rough phase diagram. We expected to find acceptable mixtures on both the Phosphate and Sulfate rich extremes. Sulfate rich mixtures are preferable because they are much less expensive. The selected mixture is similar to Sample 28.

Incongruent melting was evident as indicated by both the gradual increase in free water at the end of successive freezing cycles and the decrease in freezing temperature.

We briefly investigated three methods of mixing that were intended to minimize thermal capacity degradation due to incongruent melting. Air bubbling could not be maintained for much of the freezing cycle because the air supply was cut off due to hydrate freezing at the bubble tube outlets. Forced oil mixing also suffered from the same problem. A mechanical auger continued to work throughout the freezing cycle. The auger we used, however, did not mix the material well enough to avoid degradation. Clearly, more work must be done to improve the mixing process.

Conclusions from the mixed hydrate tests are as follows:

- A nucleating agent must be added to stabilize and minimize supercooling. Supercooling was reduced to an acceptable 2°F. Too much nucleator may interfere with complete freezing. We settled on 3% borax that is in agreement with studies by other investigators.
- Some salt settling occurs with the selected mixture. A loss of thermal capacity of about 5% must be tolerated in the design of the Energy Shaver due to this settling.
- Mixing or other corrective measures will be needed to maintain long-term thermal performance.

## 4 Feasibility Analysis

### 4.1 Technical/Commercial Feasibility

The modeling and test results indicate the technology is feasible and that the Energy Shaver could provide substantial benefit in a replacement scenario. In a replacement scenario, smaller units augmented with the Energy Shaver replace larger units. The user would see immediate cost savings from reduced demand charges and energy consumption.

It is also possible that the smaller units with the Energy Shaver could have a lower first cost. Typical pricing for small air conditioners is between \$1,000 and \$1,200 per ton. If the Energy Shaver is priced less than \$1,000, a 3-ton air conditioner with an Energy Shaver would cost less than a 4-ton air conditioner.

The Energy Shaver has the potential for being economically packaged. The salt and plastic housing are inexpensive, and the controls are simple and use existing components. Installation is simple, and in a replacement scenario the additional cost of installation would be a small part of the total.

The Energy Shaver would have an enormous impact on the California's energy consumption if it were widely implemented. Most of California has weather that is suitable for using the Energy Shaver and the largest growth areas, which are warmer inland areas, are particularly well suited for it.

In summary, the results of this effort have supported the development of a new product that can substantially benefit the California taxpayer.

## 4.2 Follow-on Development

The findings of this effort definitely support follow-on development. There are two major areas requiring further development to successfully mature the technology and bring it to market.

First is mixing of the salt hydrate to ensure repeatable, long-term performance. A low cost mixing approach must be developed that is compatible with the configuration limitations of the low cost embodiment. Second is the final packaging that enables the Energy Shaver to be integrated with new air conditioning equipment. Top priority should be given to developing the mixing approach as soon as possible. Future proposals will be submitted to the EISG Program for grants to speed development of the mixing approach.

The final step in proving the performance of the Energy Shaver is an ARI-sanctioned test. This test will be conducted as soon as practical after development of the mixing approach and final configuration is complete.